Progress in Polymer Science 156 (2024) 101871

Contents lists available at ScienceDirect

Progress in Polymer Science

journal homepage: www.elsevier.com/locate/progpolymsci

Photoiniferter polymerization: Illuminating the history, ascendency, and renaissance[☆]

Rhys W. Hughes[1], Megan E. Lott[1], Rebecca A. Olson S, Brent S. Sumerlin[*]

George & Josephine Butler Polymer Research Laboratory, Center for Macromolecular Science & Engineering, Department of Chemistry, University of Florida, PO Box 117200, Gainesville, FL 32611-7200, United States

ARTICLE INFO

Article history:
Received 3 June 2024
Revised 1 August 2024
Accepted 16 August 2024
Available online 20 August 2024

Keywords:
Controlled radical polymerization
Reversible-Deactivation radical polymerization
Photopolymerization
Photoiniferter

ABSTRACT

In this perspective, we explore the historical evolution, photochemical processes, and distinct utility of photoiniferter polymerization. We aim to provide a practical guide encompassing the selection of iniferter and monomer, coupled with the optimization of light wavelengths to conduct efficient photoiniferter polymerizations. We delve into the impact of iniferter structure on photophysical properties and the resulting polymerization behavior. Furthermore, we highlight ongoing research efforts employing photoiniferter polymerization, emphasizing its potential applications in cutting-edge areas of research such as 3D printing and the synthesis of ultra-high molecular weight polymers ($\geq 10^6$ g mol^{-1}). Through this perspective, we aim to clarify both the fundamental principles and the practical considerations of photoiniferter polymerization, ultimately advancing its utility and paving the way for innovative applications in polymer science.

1. Introduction

Ciamician, a pioneer in photochemistry, proposed in 1912 that visible light could become the resource of the future, particularly for mediating complex chemical reactions [1]. Light provides many appealing advantages for chemical synthesis compared with thermally induced reactions, e.g., spatial and temporal control [2–6]. The photoiniferter process utilizes the advantages of light-mediated reactions for polymer synthesis and advanced material design [7,8]. Photoiniferter polymerization is a light-mediated radical polymerization that traditionally employs a thiocarbonylthio compound that can harness the energy provided by light to facilitate radical initiation, chain growth, and polymerization control [9,10]. Specifically, the thiocarbonylthio compound partakes in *ini*tiation, degenerative chain trans*fer*, and reversible *ter*mination (*iniferter*) and is crucial to the success of the chemistry.[7] (Note: Although the latter process is well known as “reversible termination,” in light of IUPAC guidance suggesting “termination” be reserved to describe reactions where chain carriers are irreversibly converted to non-propagating species, we have elected to refer to the reaction of a thiocarbonylthiyl radical with the propagating chainend as “reversible combination.” This terminology is intended to prevent confusion, as the IUPAC-recommended term of “reversible deactivation” could also describe the degenerative transfer reaction.)

The phenomenon and model for reversible–deactivation radical polymerization (RDRP) was first proposed by Takayuki Otsu and his colleagues [11,12] at a time when the polymer chemistry community was investigating the complex nature of initiation and the impact of radical generation on chain-growth polymerization [13]. It was reasoned that the idea of uninterrupted radical chain growth would confer great synthetic utility, enabling the synthesis of sophisticated macromolecules with complex architectures and sequences [12,14–17]. Implementing conditions that prevented

---

[☆] ***Acronyms***: atom transfer radical polymerization (ATRP), bond dissociation energy (BDE), chain transfer agent (CTA), chain transfer constant (C_{tr}), highest-occupied molecular orbital (HOMO), less-activated monomers (LAMs), lowest-unoccupied molecular orbital (LUMO), methyl acrylate (MA), methyl methacrylate (MMA), molecular weight distribution (MWD), more-activated monomers (MAMs), nitroxide mediated polymerization (NMP), photo-electron/energy transfer-RAFT (PET-RAFT), polymerization-induced self-assembly (PISA), poly(methyl acrylate) (PMA), propagation rate constant (k_p), quantum chemical (QC), rate of initiation (R_i), rate of polymerization (R_p), reversible addition—fragmentation chain-transfer (RAFT), reversible–deactivation radical polymerization (RDRP), rate constant of chain transfer (k_{tr}), single-unit monomer insertion (SUMI), size-exclusion chromatography (SEC), styrene (St), switchable RAFT agents (SRAs), termination rate constant (k_t), three-dimensional (3D), transmission electron microscopy (TEM), triflic acid (TfOH), ultra-high molecular weight (UHMW), ultra-violet (UV).

[*] Corresponding author at: George & Josephine Butler Polymer Research Laboratory, Center for Macromolecular Science & Engineering, Department of Chemistry, University of Florida, Gainesville, Florida 32611, United States.

E-mail address: sumerlin@chem.ufl.edu (B.S. Sumerlin).

[1] The authors declare no competing financial interest.

https://doi.org/10.1016/j.progpolymsci.2024.101871
0079-6700/

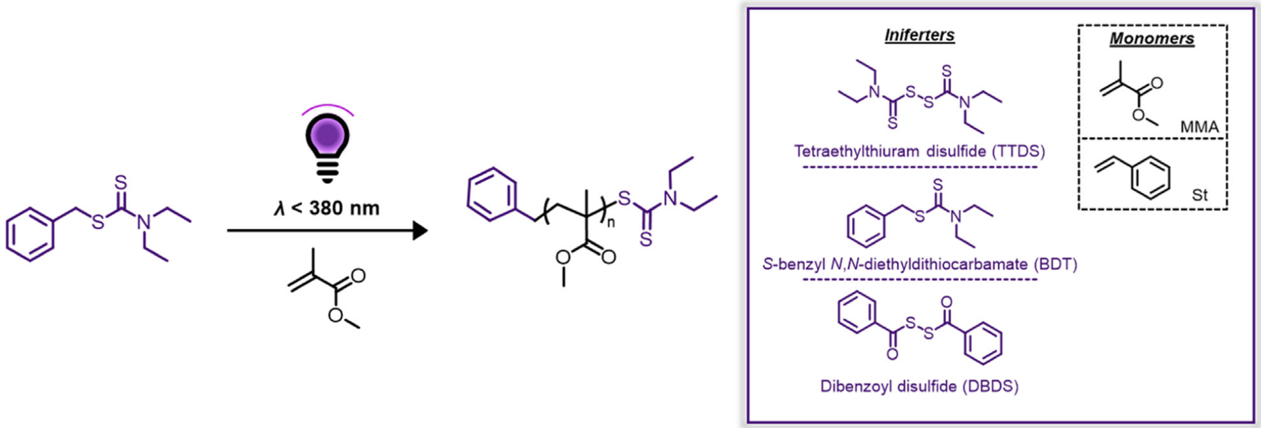

Fig. 1. Scheme of Otsu and coworker's first photoiniferter polymerizations with methyl methacrylate and styrene under UV irradiation. A linear relationship between M_n and monomer conversion was reported with these reactions, satisfying one of the facets of a controlled polymerization.

irreversible termination events became the foundation in building a model for living polymerization, first reported through anionic polymerization conditions by Szwarc in 1956 [13]. Kennedy, shortly thereafter, reported on carbocationic polymerization using initiator-transfer agents (inifers) [18]. The polymerization used alkyl halides like cumyl chloride, along with a Lewis acid such as boron trichloride which acts as the inifer for the cationic polymerization [19,20]. Sequentially, Otsu's proposed "living" radical polymerization using an iniferter was originally achieved by using a thiocarbonylthio compound which dissociated via thermal or photo-stimulus. Dissociation of the iniferter generated one radical that was reactive enough to initiate polymerization and another less reactive (persistent) radical that could prevent irreversible termination. The less reactive persistent radical was proposed to partake in reversible combination with the growing polymer chain to reduce the rate of undesired radical-radical coupling. Additionally, the thiocarbonylthio end-group was credited with enhancing the uniform growth of polymer chains via degenerative chain transfer [11]. Since bimolecular termination events are suppressed rather than a total absence of termination, photoiniferter polymerization has become known as a controlled polymerization rather than a true living polymerization.

Classic parameters of RDRP include 1. first-order kinetic behavior that indicates constant radical flux throughout the course of the reaction; 2. tunable molecular weights that are based on reaction stoichiometry and monomer conversion; 3. designed (usually narrow) molecular weight distributions; 4. polymer chain-end fidelity that allows for successful chain extensions [17]. Otsu was able to partially demonstrate the classic parameters of RDRP in 1982 via a seminal publication where thermal iniferter polymerization of methyl methacrylate (MMA) and styrene (St) and photoiniferter polymerizations of MMA and St under ultra-violet (UV) irradiation was demonstrated (Fig. 1) [11].

Although understanding of RDRP has grown exponentially since this first report and many more RDRP methods have been reported since (including: nitroxide mediated polymerization (NMP) [21–24], atom transfer radical polymerization (ATRP) [25–31], reversible addition—fragmentation chain-transfer (RAFT) polymerization [15,32–39], etc.), the versatility of photoiniferter polymerization is evidenced by its resurgence in recent years [28,40–46]. We notice that the information pertaining to this topic can be vast, making it daunting to newcomers; as such, we find this perspective timely in light of the vast amount of literature that pioneers this polymerization process. Features such as the photochemistry and electronic behavior of thiocarbonylthio compounds under irradiation are pertinent to understanding the polymerization mechanism and accurately interpreting results derived from photoiniferter polymerizations. Detailed compatibility of various photoiniferters with vinyl monomers to achieve polymers with low-to-moderate dispersity will also be explored, in addition to the applications of this polymerization approach. Thus, the primary goal of this perspective is to effectively introduce photoiniferter polymerization to a broader audience and facilitate its adoption by the greater scientific community.

2. Photoiniferter and raft polymerization

The concept of a photoiniferter polymerization remains unchanged from Otsu and coworker's initial reports with dithiocarbamates [47]; however, immense progress has been made towards improving polymerization control. The word "photoiniferter" clearly communicates both the role of the molecule during polymerization and the stimulus applied for the homolytic dissociation that provides the radicals needed for initiation and propagation. In photoiniferter polymerization, an electron in the iniferter is excited by the absorbance of light. The absorbance of light due to the C=S bond facilitates β-scission of the neighboring C—S bond which connects the R-group to the thiocarbonylthio moiety. Cleavage of the C—S bond generates a carbon-centered radical and another less reactive thiocarbonylthio radical (Fig. 2). The carbon-centered radical is proposed to initiate polymerization by reacting with monomer, while the thiocarbonylthiyl radical is capable of reversible combination to deactivate growing polymer chains [48]. Photoiniferter polymerization is also regulated by a degenerative chain transfer process where a radical on a growing polymer chain is transferred to a dormant polymer chain bearing a thiocarbonylthio chain end. Rapid transfer of the polymeric radical activates the dormant chain and deactivates the growing polymer chain, allowing for the uniform growth of all polymer chains over the course of the polymerization [49]. The contribution of each mechanism is dependent on the choice of iniferter and monomer, and is discussed in Section 5.

Due to the participation of a thiocarbonylthio species and a mechanism of degenerative chain transfer as a form of control within a photoiniferter polymerization, many publications have associated photoiniferter polymerization with RAFT polymerizations, using terminology such as "Photo-RAFT" or "Photoiniferter-RAFT." However, the originally proposed mechanism of RAFT polymerization requires the use of an exogenous initiator, which is usually dissociated using heat, and its thiocarbonylthio species is proposed to only participate in degenerative chain transfer and does not participate in reversible combination (Fig. 2) [50–53]. Thus,

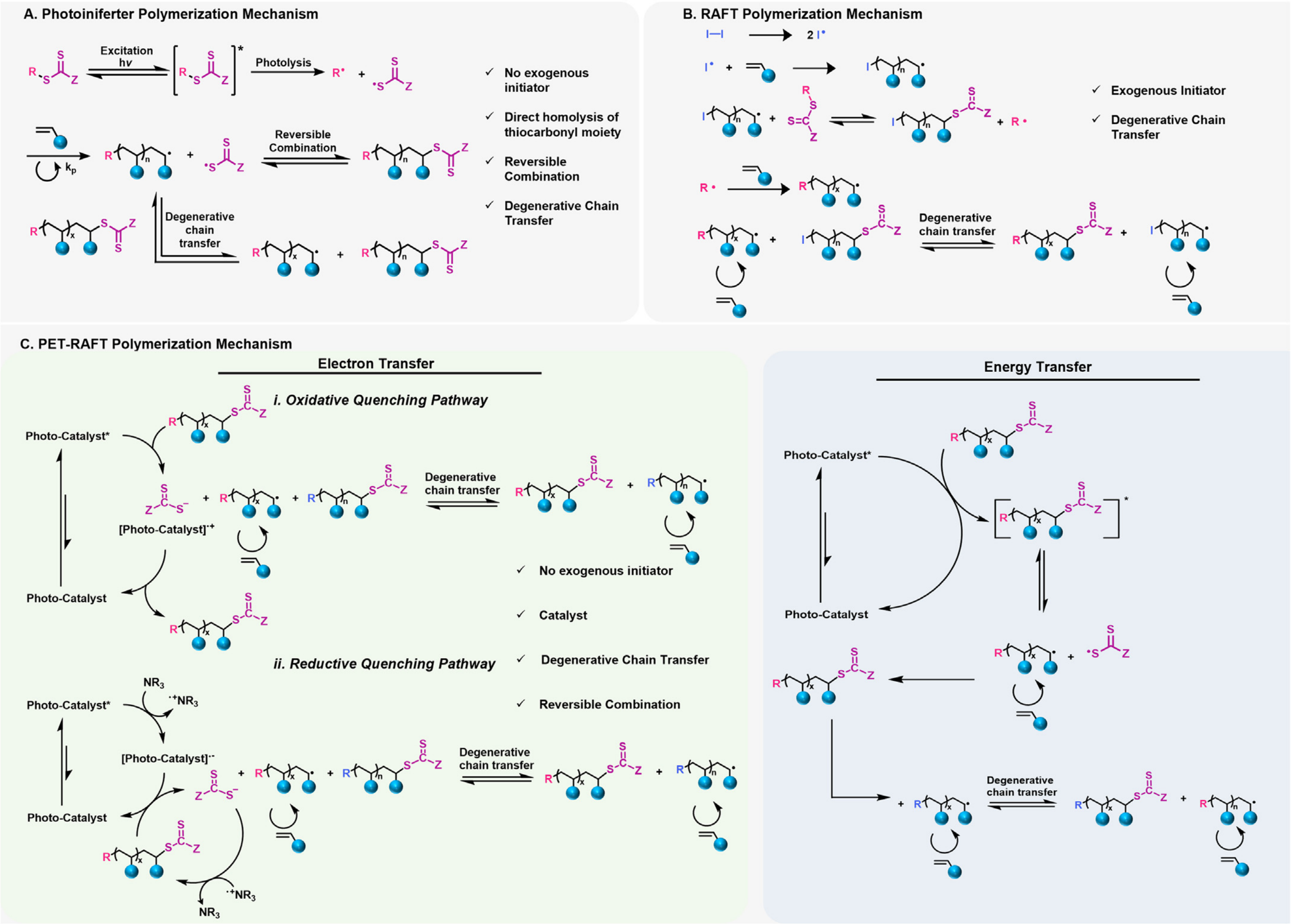

Fig. 2. The mechanisms of (A) Photoiniferter polymerization, (B) RAFT polymerization, and (C) PET-RAFT polymerization.

the thiocarbonylthio species in a RAFT polymerization is more appropriately termed a chain transfer agent (CTA). Photoinitiated-RAFT is a common adaptation of conventional RAFT polymerization, whereby the exogenous initiator is photoactivated (i.e., a photoinitiator) [54,55]. Therefore, the presence of an exogenous initiator excludes categorization as a photoiniferter polymerization.

A more complicated distinction is between photoiniferter polymerization and photo-electron/energy transfer-RAFT (PET-RAFT) polymerization. PET-RAFT polymerization involves the use of a photocatalyst that is excited by light and transfers an electron/energy to the thiocarbonylthio moiety [56]. PET-RAFT can proceed by both an oxidative and reductive catalytic mechanism to confer high degrees of control over the polymerization (Fig. 2). Given the presence of a catalyst, PET-RAFT has more flexibility to fine-tune the irradiation wavelength, whereas photoiniferter requires absorption of light directly by the thiocarbonylthio species [57]. However, under particular wavelengths of light, the thiocarbonylthio unit in a PET-RAFT polymerization can undergo the same three mechanistic aspects of the photoiniferter process, but the presence of an exogenous catalyst in PET-RAFT polymerization has generally precluded its classification as a photoiniferter polymerization. Another mechanistic consideration with PET-RAFT polymerization is since the exogenous catalyst transfers an electron/energy to the thiocarbonylthio functionality and the thiocarbonylthio molecule also participates in reversible combination, it has been suggested that an alternative descriptor could be photo-electron/energy transfer-iniferter (PET-iniferter) polymerization, as proposed by Johnson and coworkers [3].

The absence of exogenous initiator in photoiniferter polymerization has been proposed to potentially lead to more well-defined polymers with narrower dispersities when compared to polymers prepared via RAFT polymerization. Recent work by Kwon et al. elucidated the fraction of dead chains during the synthesis of poly(methyl acrylate) (PMA) by photoiniferter polymerization and RAFT polymerization. The photoiniferter polymerization led to ~3% of dead chains, which was determined by UV–vis analysis, while the corresponding RAFT polymerization led to a much larger fraction of dead chains at 15% despite having a slower rate of polymerization [58]. This level of control in photoiniferter polymerization has allowed for the synthesis of controlled ultra-high-molecular weight (UHMW, 10^6 g mol^{-1}) polymers with narrow dispersities by using this approach [59–61].

3. Iniferter classification

3.1. Classification by stimulus

Iniferters can be classified by symmetry and the stimulus applied to trigger homolytic cleavage (Fig. 3) [12]. Otsu et al. had documented cases of thermal, photo, and redox iniferters which all followed the proposed model for “living” radical polymerization [12,62,63]. Thermal iniferters undergo dissociation of a weak

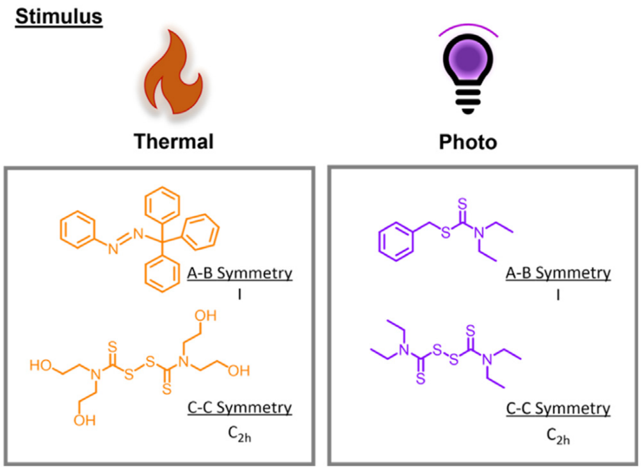

Fig. 3. Various methods of iniferter classification based on the stimulus used for iniferter dissociation and symmetry.

bond triggered by heat (such as a disulfide bond, bond dissociation energy (BDE) ≈ 16 kcal/mol) [64,65]. A photoiniferter polymerization most commonly uses a thiocarbonylthio compound that undergoes photolysis of the C—S bond by β-scission upon irradiation. Both thermal and photoiniferters are single molecules that generate two radicals after dissociation initiated by a stimulus and are still relevantly termed iniferters. Redox iniferters consisted of two-components and were based on the redox reaction of nickel (Ni^0) with an organic halide (R—X), such as benzyl chloride, to form the benzyl radical, which can initiate polymerization. The oxidized Ni complex and C—X bond at the chain-end further engage in a reversible combination mechanism to control chain growth [14]. Redox iniferters do partake in initiation and reversible combination; however, since degenerative chain transfer is not expected, we find that this previously classified term is outdated and does not fit the current criteria of an iniferter. Among these various classification types, it is also important to note that the synthetic relevance of thermal and redox iniferters has diminished, largely due to the later discovery of RAFT polymerization and ATRP [28,32,34,56,66]. In a similar fashion, ATRP also uses transition metal catalysts which react with a dormant alkyl halide to form a carbon centered radical capable of propagation and an oxidized transition metal complex which can then deactivate the growing polymer chain [67,68].

3.2. Classification by symmetry

Iniferters can be categorized as symmetrical C–C types (possessing higher-order symmetry elements such as C_2) and unsymmetrical A–B types (only containing the universal symmetry element- C_1/I) (Fig. 3) [12]. Due to the symmetric nature of C–C iniferters, two identical relatively stable radicals are generated upon homolytic bond cleavage. This approach tends to result in polymers with high dispersities as a consequence of inefficient initiation [12,63,69]. By adjusting the intensity of the applied stimulus, the rate of iniferter dissociation can be tuned to obtain polymerizations with varying levels of control [70]. Perrier and coworkers used this method with symmetrical bis(trithiocarbonate) disulfides, reporting that higher energy blue light resulted in increased photodegradation rates and poorer control during polymerization of MMA, as compared to the same polymerization carried out under green light. Alternatively, the polymerization of methyl acrylate (MA) using these iniferters was inhibited under green light and required conditions that more strongly favored initiation. The inhibition of MA polymerization was caused by the increased stability of the R-group after monomer addition, which reduced the rate of iniferter reactivation [70].

The common drawbacks associated with C–C iniferters can also be resolved using unsymmetrical A–B iniferters. In this case, the A radical is tuned to be more reactive towards addition to monomer to promote rapid initiation (crucial for low dispersity), while the B radical is much less/non-reactive towards monomer initiation and primarily participates as a control agent during the polymerization via reversible combination [14]. The lack of symmetry in A–B-type iniferters enables the synthesis of polymers with predictable molecular weights and architectures. As a result, asymmetric A–B type iniferters are now employed most commonly.

4. Photochemistry of Photoiniferters

Successful photoiniferter polymerizations hinge on light absorption and electronic excitation for efficient photolysis [57]. Key factors such as light intensity, wavelength, and the specific iniferter employed play pivotal roles in shaping the outcome of photoiniferter polymerization. We thus seek to consider these concepts from a photophysical point of view to obtain an understanding of the photochemical processes that result.

4.1. Light intensity

Every chain polymerization is comprised of an initiation, propagation, and termination step. In thermal polymerizations, thermal radical initiators decompose when exposed to a given temperature to generate radicals that initiate polymerization. The obtained rate of initiation (R_i) can be defined by the Arrhenius equation, $R_i = A_i \times e^{-\frac{E_{a,i}}{RT}}$, where A_i represents the pre-exponential factor for initiation, $E_{a,i}$ is the activation energy for initiation, R is the universal gas constant, and T is temperature in Kelvin [17,71]. Through this equation, it is found that increasing temperature results in an increase in R_i due to a higher quantity of initiator molecules at or above the activation energy required for decomposition. Simply put, in thermal polymerizations radical generation and therefore R_i (and the resulting overall polymerization kinetics) can be tuned through temperature. In photoiniferter polymerization, light intensity can also be altered to tune radical generation and R_i. In photo-initiated polymerizations, R_i can be defined by the following equation, $R_i = \phi \times I$, where ϕ is the quantum yield (which represents the efficiency of radical generation per absorbed photon) and I is the intensity of light (photons per unit area per unit time) [71]. In this case, a higher light intensity will result in an increase in R_i. By assuming steady state kinetics where the rate of initiation is equal to the rate of termination, we can determine the effect of light intensity on the rate of polymerization. Given that the rate of polymerization (R_p) equation is $R_p = k_p[M][P^*]$ (k_p is the rate constant for propagation, [M] is monomer concentration, $[P^*]$ the concentration of active propagating radicals and $[P^*] = \sqrt{\frac{2fk_d[I]}{k_t}}$ (where f is the efficiency of initiator decomposition, k_d is the rate constant for initiator decomposition, [I] is the concentration of the initiator, and k_t is the rate constant for termination), we can see that the $R_p \propto \sqrt{R_i}$. Since $R_i = \phi \times I$, it can be concluded that $R_p \propto \sqrt{I}$. Amongst others, Johnson and coworkers observed that using higher light intensities led to faster polymerizations [72,73]. For example, using a difunctional trithiocarbonate for the polymerization of *N*-isopropylacrylamide, it was observed that higher intensity light generated more radicals which predictably led to faster polymerizations. However, the increased rate of polymerization came at the expense of control, likely due to the increased generation of radicals in solution causing more irreversible termination events (the same phenomena observed when increasing temperature in thermal polymerizations).

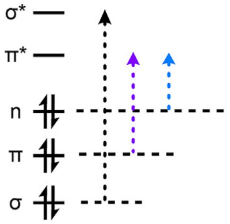

Fig. 4. Displaying the electronic excitations available using thiocarbonylthio molecules.

Increased dispersities at higher light intensities evidenced the decrease in control of polymerization. Further in this study, lower light intensities afforded polymerizations with the best control.

4.2. Light wavelength

Light wavelength is an essential consideration in photoiniferter polymerizations, as it can be used to target specific electronic excitations, leading to differences in polymerization outcomes. To achieve effective iniferter photolysis, the chosen wavelength of light is usually aligned with the absorbance of the iniferter. However, recent reports by Barner-Kowollick have demonstrated through the use of action plots that the wavelength of a molecules absorbance and the wavelength at which reactivity is optimized can be vastly different [74–76]. For photoiniferter polymerization, when the iniferter absorbs energy from light, typically UV or visible light, electronic excitation occurs, and an electron is promoted from its ground state to a higher energy state. Determining whether an electronic excitation is possible is dependent on adherence to the electronic selection rules, which state:

- The total spin for an electronic excitation cannot change, i.e., $\Delta S = 0$ [77].
- The change in total orbital angular momentum $\Delta L = 0, \mp 1$ this is the La Porte rule but only applies to molecules that have an inversion center [78].
- The change in total angular momentum can be $\Delta J = 0, \mp 1$.
- The initial and final wavefunctions must change in parity.

Electronic transitions that obey selection rules will display strong absorbance by UV–vis spectroscopy and can be quantitatively described through extinction coefficients. The extinction coefficient is a measure of how likely an electronic transition is to occur, i.e., electronic transitions that obey the electronic selection rules will display large extinction coefficients ($\varepsilon \sim 10{,}000\ M^{-1}\text{cm}^{-1}$). Practically, the lower extinction coefficient means that fewer excitation processes occur, potentially altering excitation/relaxation pathways and thereby affecting the quantity of generated radicals—a critical factor in governing the polymerization process. The nature of the solvent is also important, with polarity affecting the energy of the electronic transitions that dictate photochemistry.

4.3. Electronic transitions

In molecular orbital theory, the electronic transitions can be thought of as exciting an electron from a bonding or non-bonding orbital into an antibonding orbital [79]. The following excitations are possible: $\sigma\rightarrow\sigma^*$, $\pi\rightarrow\pi^*$, n→π^*, and n→σ^* (Fig. 4) [80]. Due to the high energies required for excitation to the σ^*, these electronic transitions are not usually targeted. Classically targeted excitations in photoiniferters are the $\pi\rightarrow\pi^*$ and the n→π^*. These excitations appear in the UV or visible region, making them highly accessible with simple photoreactor setups [81]. The $\pi\rightarrow\pi^*$ transition leads to excitation of an electron from the C=S π-bond into the analogous antibonding orbital, while the n→π^* transition involves excitation of an electron from a lone pair on the sulfur atom of the C=S bond, into the C=S π-antibonding orbital. Excitation of an electron from the π-orbital to the π^*-orbital in thiocarbonylthio photoiniferters requires around 300 nm light, the extinction coefficient for this transition is large due to agreement with the electronic selection rules (Fig. 4) [82].

The energy difference between the n and the π^* orbitals is smaller than that for the $\pi\rightarrow\pi^*$, and consequently requires longer wavelength light to access [83]. As a result of the lower energy light required, it is hypothesized that excitation occurs from S_0 to the first excited singlet state (S_1), and then proceeds to the first excited triplet state (T_1) by intersystem crossing due to the small energy gap between S_1 and T_1 [82]. Thus, the change in spin associated with the n→π^* transition results in a much lower extinction coefficient compared to that of the $\pi\rightarrow\pi^*$. Once excited, the iniferter can proceed via one of 3 pathways: 1. return to the ground state by radiative processes such as fluorescence or phosphorescence; 2. by non-radiative pathways; or 3. lead to a photochemical reaction [84].

Additional mechanistic insights of these electronic excitations were further reported on by Kwon, et al. though quantum chemical (QC) calculations and polymerizations [57,58]. While certain photoiniferter polymerizations lacked control at room temperature when targeting the n→π^* transition, heating improved molecular weight control. This report suggests heating light-mediated polymerizations can overcome potential activation barriers involved in photolysis.

The quantum yields of thiocarbonylthio molecules also remain largely unexplored, though excitation of the n→π^* transition has been shown to lead to faster photolysis than when targeting the $\pi\rightarrow\pi^*$ transition of trithiocarbonates and xanthates.^{6} The fact that lower energy light can be used is appealing and could be important where light sensitivity is considered.

While all these reports offer valuable mechanistic insights, the precise comprehension of the photochemical processes involved in photoiniferter polymerization remains incomplete. Interdisciplinary research methods are actively addressing this shortcoming of understanding.

4.4. Influence of iniferter R- and Z-Group on photochemistry

Targeting various transitions with different photoiniferters can result in distinct outcomes on the control of the polymerization, since the wavelength of light required to target these electronic excitations is highly dependent on the iniferter structure (Fig. 5A). The $\pi\rightarrow\pi^*$ transitions of all iniferters are similar in excitation wavelength, appearing between 270 and 320 nm (Fig. 5B); however, the iniferter structure greatly affects the location of the n→π^* transition (Fig. 5C) [85]. The iniferter structure can be divided into R-group and Z-group effects. First, we will discuss the Z-group effects, since the effects on wavelength absorbance are more pronounced.

The four common classes of thiocarbonylthio photoiniferters are trithiocarbonates, dithiobenzoates, xanthates, and dithiocarbamates (Fig. 5A). The $\pi\rightarrow\pi^*$ transition for most trithiocarbonates appears at ~310 nm, while the n→π^* transition requires less energy for excitation and generally arises at ~450 nm [33,86]. The n→π^* excitation of trithiocarbonates is responsible for the color of the iniferter, and since most trithiocarbonates absorb in the blue region of the visible spectrum, they appear yellow-orange.

Dithiobenzoates absorb green light and appear red due to the absorbance of the n→π^* transition, which is located at much longer wavelengths, than observed for other iniferters because of the increased conjugation [87–92].

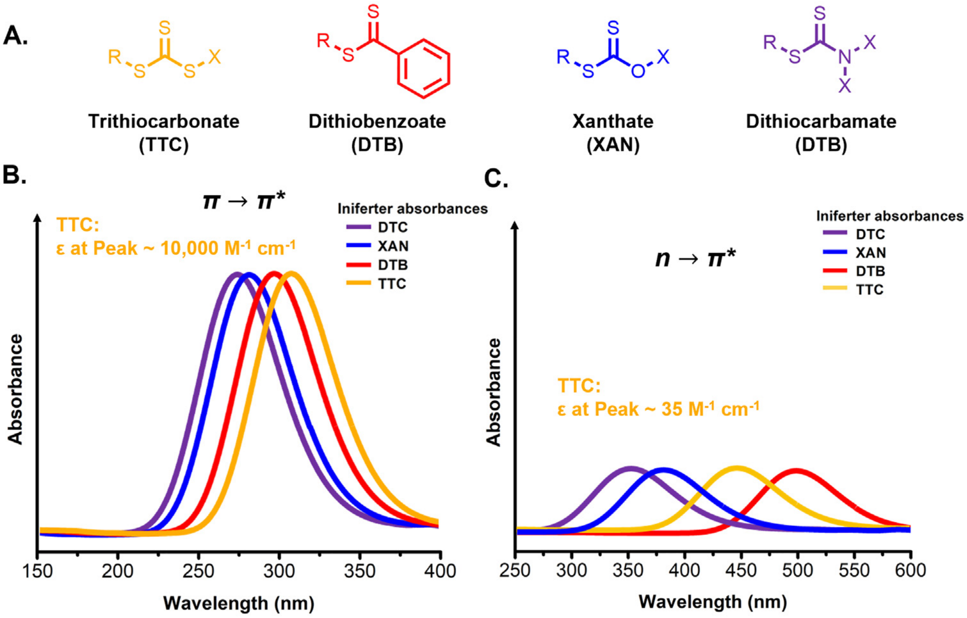

Fig. 5. (A) General structure of common iniferters used in photoiniferter polymerization. (B) Representation of the $\pi \rightarrow \pi^*$ transitions for the respective iniferters. (C) Representation of the of $n \rightarrow \pi^*$ transition for the respective iniferters.

Xanthate excitations are observed at shorter wavelengths, because of the electron-donating oxygen atom adjacent to the C=S bond resulting in larger HOMO-LUMO gaps than are found for trithiocarbonates [59]. The resulting increased energy gap is evidenced by the shift in absorbance for photoexcitations to higher energy. The $\pi \rightarrow \pi^*$ transition of xanthates is found around 280 nm while the $n \rightarrow \pi^*$ excitation is hypsochromically shifted to 365 nm [10,93]. Dithiocarbamate photoexcitations are also shifted to shorter wavelengths due to the increased donating ability of the nitrogen atom, leading to a $\pi \rightarrow \pi^*$ absorbance of around 280 nm (Fig. 5) [44]. The ability to target specific electronic excitations across the visible and UV regions by careful selection of photoiniferter structure is a key benefit of this polymerization method and may prove particularly useful when conducting polymerization in the presence of sensitive biological (macro)molecules [4,49,94].

The different Z-groups of iniferters control not only the wavelength of light required to target electronic excitations but also the rate of photolysis. Photolysis of xanthates has been demonstrated to be much faster than that of trithiocarbonates. The accelerated rate of photolysis can be attributed to the increased resonance donating effect of the oxygen atom in xanthates causing a lower bond dissociation energy of the C—S bond (38.1 kcal/mol)[95] compared to that of trithiocarbonates (41.5 kcal/mol) [10,95].

Qiao and coworkers among others have demonstrated that the rate of initiation during photoiniferter polymerization is dependent not only on the Z-group of the iniferter, but also on the nature of the R-group formed upon photolysis [96,97]. Common R-groups of photoiniferters are shown in Fig. 6. Trithiocarbonate iniferters with R-groups that cleave to form less stabilized radicals suffer from slow initialization due to a slow rate of iniferter photolysis. Interestingly, more stabilized R-group radicals such as those generated on tertiary-cyano-functionalized groups demonstrate limited inhibition. These findings suggest the rate-determining step for photoiniferter initiation is the rate of C—S photolysis and not the sequential rate of radical addition to monomer (i.e., reinitiation). Although slow initialization is often observed with iniferters that cleave to form less stabilized R-group radicals, the polymerizations can be controlled due to the high-chain-transfer capability of the trithiocarbonate. To remedy the slow initiation observed for R-groups which form less stabilized radicals, a higher light intensity can also be used to accelerate photolysis.

The monomer being polymerized also needs to be taken into consideration when conducting a photoiniferter polymerization since photolysis of a polymer bearing an iniferter may be different than the original iniferter. A monomer which generates a stable radical will in most cases permit efficient photolysis; however, a monomer unit which takes on the structure of a poor “R” group upon homolysis will hinder photolytic cleavage during polymerization.

5. Matching monomers to iniferters

In addition to matching the iniferter to the wavelength of light used during polymerization, it is important to consider the monomer being polymerized [9,16,17,98]. Iniferter-monomer pairing will affect the rates of β-fragmentation during the initialization period and degenerative transfer during polymerization. Moreover, while a considerable body of literature prescribes CTA selection during RAFT polymerization [99,100], the effect of photolysis and reversible combination must also be considered during photoiniferter polymerization. The discussion that follows highlights examples from the literature that aid in identifying iniferters for the polymerization of common classes of vinyl monomers.

5.1. Degenerative chain transfer vs. reversible combination

Deactivation of the propagating radical can occur by both degenerative chain transfer and reversible combination. When combined with photolysis, the rates at which these reactions occur influence the rate of polymer deactivation and determine the level of molecular weight control during polymerization. To achieve rapid initiation, it is important to consider the R-group radical stability (Fig. 7A). Enhanced stability of the R-group radical allows for efficient β-fragmentation of the iniferter to the R-group, which facilitates rapid consumption of the iniferter and the uniform growth of polymer chains. In consequence, an iniferter that fragments to create stable R-group radicals, such as those stabilized by the captodative effect, promotes efficient β-fragmentation [101]. As in the

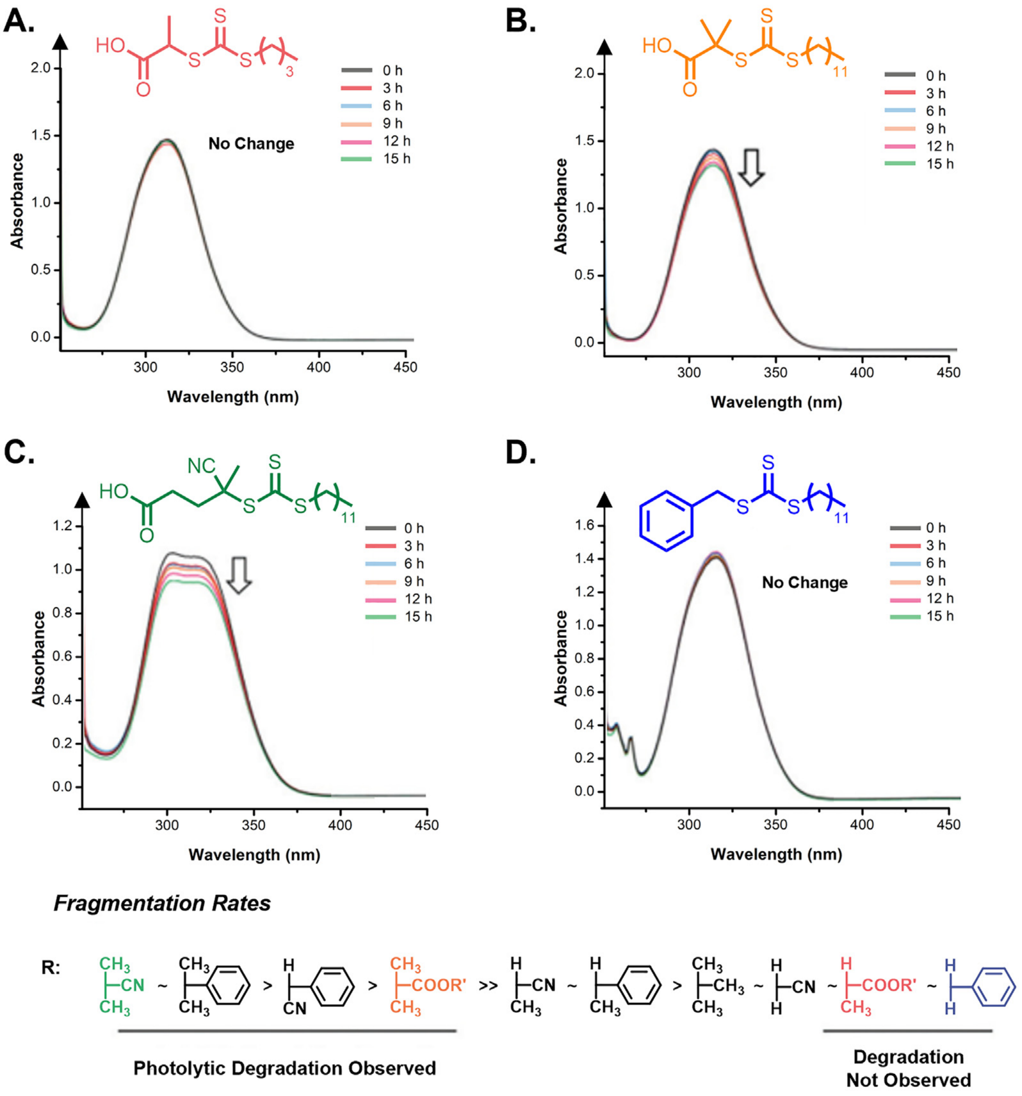

Fig. 6. UV–vis spectra displaying trithiocarbonate photodegradation with respect to time. Adapted with permission from Reference [97]. Copyright© 2016, Royal Society of Chemistry.

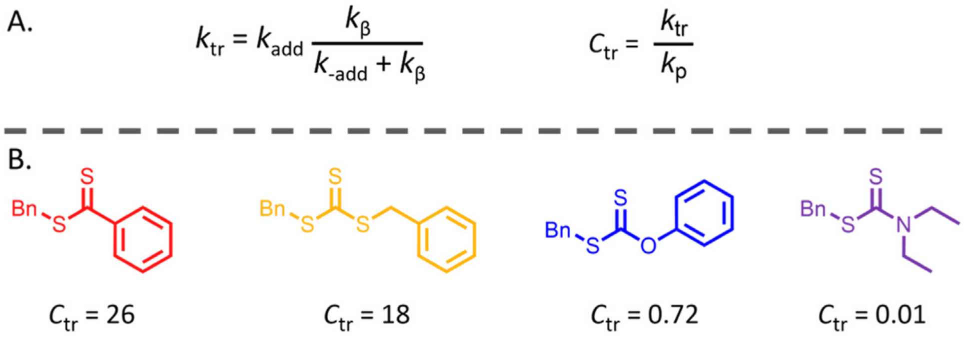

Fig. 7. (A) Equation for the chain transfer constant. (B) Chain transfer constants of common iniferters in styrene at 110 °C, Bn = Benzyl [42]. Adapted with permission from Reference [42]. Copyright© 2000, John Wiley and Sons.

case of RAFT polymerization, the stability of the R-group radical that results after either β-fragmentation or photolysis of the photoiniferter can also affect the rate of reinitiation, further emphasizing the importance of considering the relative stability of the R-group radical compared to the propagating chain end.

The degree of degenerative chain transfer and reversible combination that a polymerization undergoes can be evaluated by considering radical stabilities and chain transfer constants (Fig. 7, 9). Common monomers that yield relatively stable propagating radicals include acrylamides, acrylates, methacrylates, and styrenics (i.e., "more-activated monomers" (MAMs)). MAMs are typically paired with an iniferter with a high chain-transfer constant (C_{tr}) such as trithiocarbonates and dithiobenzoates (Fig. 9A, Fig. 9B) [34,66,102]. C_{tr} is defined as the ratio of the rate con-

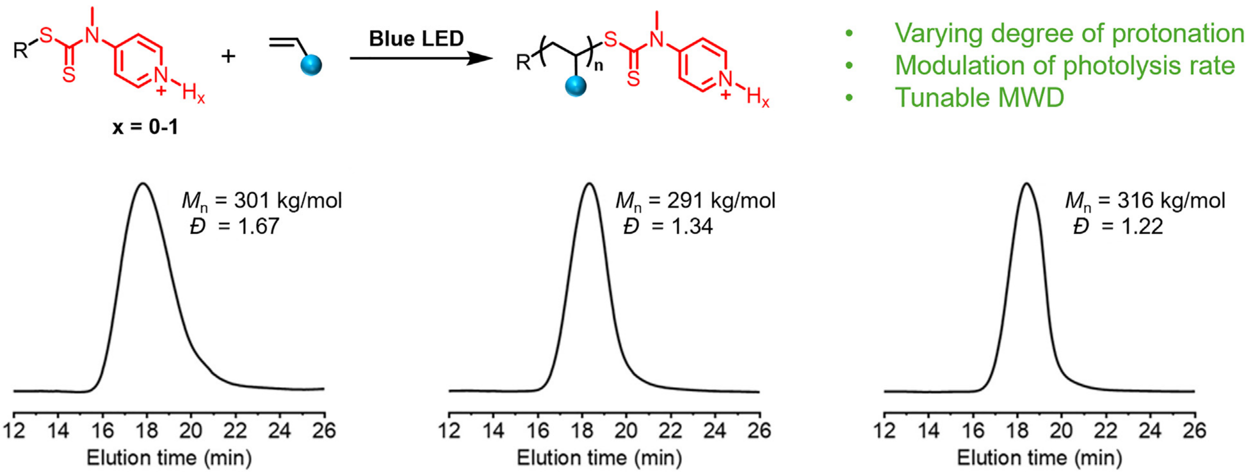

Fig. 8. (A) Generic polymerization scheme with varying degrees of protonation of the switchable RAFT agents (SRAs) to tune activities. (B) Size-exclusion chromatography (SEC) traces of polymers obtained from photoiniferter polymerization using different amounts of triflic acid (TfOH) to protonate the switchable raft agent. Adapted with permission from Reference [109]. Copyright© 2023, John Wiley and Sons.

stant of chain transfer (k_{tr}) to the k_p (Fig. 7A). The very high C_{tr} of dithiobenzoates and trithiocarbonates during polymerizations of MAMs (Fig. 7) suggests control using these iniferters is likely dominated by degenerative chain transfer rather than photolysis. Monomers that yield less stabilized propagating radicals include vinyl esters, vinyl amides, and vinyl halides (i.e., “less-activated monomers” (LAMs)). LAMs tend to be better controlled by iniferters with low C_{tr} values, such as xanthates and dithiocarbamates (Fig. 7A, Fig. 9B) [16]. For example, while xanthates are generally poor RAFT agents for the polymerization of MAMs, employing xanthates during photoiniferter polymerization of some MAMs provides acceptable control. [10,45,103] Since the C_{tr} of xanthates with MAMs is low, it is reasonable to attribute the majority of control to reversible combination/initiation. However, the relative contributions of each deactivation mechanism in determining control during photoiniferter polymerization is still a subject of debate and highly dependent on reaction conditions [104]. This aspect of photoiniferter polymerization provides versatility with respect to iniferter and monomer combinations[85,105,106] and even allows for the synthesis of block copolymers with reversed blocking order (vide infra).

Tunable Z-groups of chain transfer agents for RAFT polymerization were first introduced by Rizzardo, Moad, and Thang [107]. By tuning the Z-group the chain-transfer constant can also be altered. Classically this has been achieved with a dithiocarbamate with a pyridine ring attached that can be protonated or deprotonated [107,108]. The Qiao group demonstrated that by controlling the degree of protonation of the pyridine ring in photoiniferter polymerization the polymer molecular weight distribution can be tuned (Fig. 8) [109]. When protonated the iniferter has a high C_{tr} and provides good control over molecular weight and dispersity during the polymerization of MAMs. When carried out under conditions where the iniferter was deprotonated, the resulting low C_{tr} of the iniferter led to poor control. These results suggest that exogenous modulation of iniferter structure is a viable strategy to tune the chain length distribution [109].

To provide guidance on matching monomer and iniferter reactivities, see Fig. 9. As discussed in earlier sections, there are multiple ways to classify a controlled polymerization, including a linear evolution of number-average molecular weight versus conversion, low dispersity, and chain-end fidelity. Fig. 9B has selected one of these parameters of a controlled polymerization, namely dispersity, to provide guidance for matching iniferters with monomers.

6. Depolymerization

While polymer degradation is potentially one way to address the accumulation of plastic waste [120–130], more recently depolymerization has risen as an attractive alternative approach [131–137]. Cleavage of the thiocarbonylthio group under irradiation can be used not only for chemical transformations but also to improve the chemical recyclability of polymers. Initial reports by Gramlich and coworkers and Anastasaki and coworkers demonstrated that poly(methacrylates) bearing labile chain-ends such as dithiobenzoates and trithiocarbonates could be activated to induce depolymerization [138,139]. Inspired by this approach, recent progress has demonstrated that the rate of depolymerization in solution can be accelerated using light in conjunction with heat to induce C—S photolysis directly[140] or with a photocatalyst (Fig. 10) [141]. Alternatively, bulk depolymerization of poly(methyl methacrylate) synthesized by photoiniferter polymerization achieved ~90% depolymerization through the cleavage of thermolytically labile end groups, the fidelity of which was ensured by photoiniferter polymerization [142].

The emerging technology of depolymerization is particularly timely, not only because of the potential for enhanced sustainability but also because the process can potentially be used to address current persisting challenges in polymer science [132,142–144]. For example, investigation into the fate of the thiocarbonylthio moiety upon depolymerization by Anastasaki and coworkers[145] led to the first reports of controlled depolymerization [146,147]. Continuing to combine depolymerization methodologies to address chemical waste is an important consideration toward a more sustainable future [148].

7. Applications of photoiniferter polymerization

Photoiniferter polymerization has been used to afford materials with improved mechanical properties, to achieve high throughput methodologies, and to provide precise control over polymer sequence. In this section, we will discuss how photoiniferter polymerization can be used to synthesize polymers with wide-reaching applications.

7.1. Ultra-high-molecular-weight (UHMW) polymers

UHMW polymers are desirable due to their robust material properties and ability to mimic many naturally occurring

A.

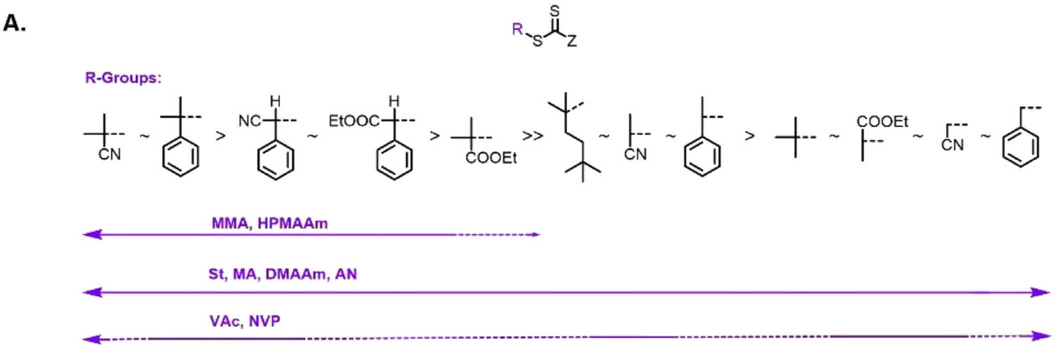

B.

	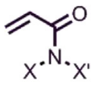	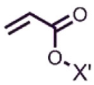	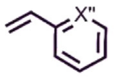	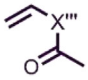	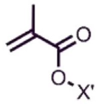
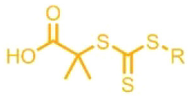	[44,61,81,110] +++	[61,73,81] +++	[81] +++		[61,111] +
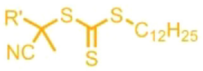		[111] +++	[112,198] +++		[113,114,198] +++
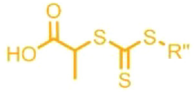	[49] +++	[49] +++			
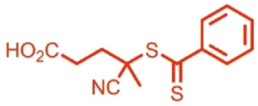		[97] -	[115] -		[97,111,114] +++
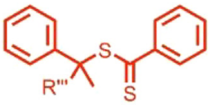			[116] +++ *+ Maleic Anhydride*		[115] +
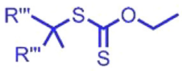	[44] +++	[117] ++		[118] ++	[10] +
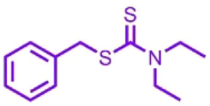			[119] +	[119] +	[119] +

Fig. 9. (A) Common R-groups on iniferters with general structure R–S–(C=S)–Z for various monomers; MMA = methyl methacrylate, HPMAM = *N*-(2-hydroxypropyl)methacrylamide, St = styrene, MA = methyl acrylate, DMAAm = dimethyl acrylamide, AN = acrylonitrile, VAc = vinyl acetate, NVP = *N*-vinylpyrrolidone. Adapted with permission from Reference [9]. Copyright© 2022, John Wiley and Sons. (B) R = $C_{12}H_{15}$ or C_3O_2H; R′ = CH_3 or C_3O_2H; R″= $C_{12}H_{15}$ or C_4H_9; R‴= CH_3 or H; R⁗= $CO_2C_2H_5$, C_2O_2H, or CN [110–119].

X/X′= alkyl groups or H; X″ = C or N; X‴ = *O* or N. Boxes intentionally left blank are due to no literature or data matching iniferter to specified monomers.

+++ = resulting polymerization dispersity of 1.00 — 1.29*

++ = resulting polymerization dispersity of 1.30 —1.49*

+ = resulting polymerization dispersity of 1.50 — 2.00*

- = substantial retardation or not achieving targeted molecular weight combined with high dispersities

*Under cited conditions

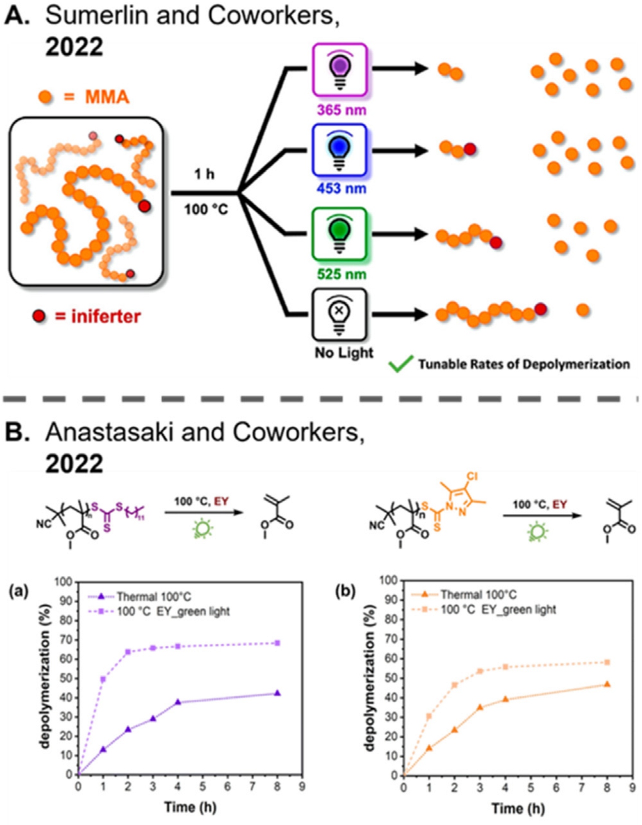

Fig. 10. Light-mediated depolymerization through (A) photoiniferter type photolysis or (B) photoredox catalyst. Adapted with permission from Reference [140] and [141]. Copyright© 2022, American Chemical Society and Royal Society of Chemistry.

biomacromolecules [59,149–151]. Often, UHMW polymers are defined as polymers of molecular weight $\geq 10^6$ g mol^{-1} [149,152]. High molecular weight polymers can be readily generated by conventional radical polymerization; however, lack of control over both molecular weight and molecular weight distributions, tied with the inability to achieve advanced architectures limits the applications of materials synthesized by this approach [149,150]. To obtain the benefits offered by UHMW polymers and expand their application, RDRP methods can be used [59,61]. There are reports on forming high molecular weight polymers via RDRP methods [153–155], however, the synthesis of UHMW polymers by RDRP has been particularly challenging [59,61,156–158]. To favor high molecular weights, monomers with high k_p and low rates of termination are desired [59]. Until recently, many of the reports synthesizing UHMW polymers have utilized high pressure, aqueous media, or ionic liquids [157,159–164] to increase k_p [165,166]. However, photoiniferter polymerization is an attractive method to synthesize polymers with predictable UHMW and low dispersity under ambient conditions [59–61,167–169]. For example, it has been reported that high/UHMW polyacrylates and polyacrylamides synthesized by photoiniferter polymerization had dramatically improved thermal, mechanical, and adhesive properties. Based on these findings, applications using these materials in pressure-sensitive adhesives have been reported [152,170]. UHMW polyacrylamides synthesized by photoiniferter polymerization are amenable to post-polymerization modification with a library of amines via transamidation of the acrylamide [168]. In addition, UHMW polymethacrylates synthesized via photoiniferter polymerization bearing pendent β-triketones have been shown to be highly reactive towards amines, with the diketoenamine product able to undergo catalyst-free dynamic transamidation in the presence of excess amines [169]. UHMW polymers synthesized via photoiniferter polymerization have also demonstrated promise as high-performance flocculants [164]. UHMW polyacrylamides synthesized via photoiniferter polymerization with a narrow molecular weight distribution (MWD) exhibited improved flocculation efficiencies compared to a commercial benchmark with a broad MWD [164].

7.2. 3D-Printing and oxygen tolerance

Photoiniferter polymerization has also been employed in a variety of 3D printing applications [171–173]. Initial reports relied on trithiocarbonates, however, slow rates of photolysis of trithiocarbonates are potentially detrimental to large-scale open-to-air methods [174]. Despite trithiocarbonates being the most widely used thiocarbonylthio compounds for photoiniferter polymerization, xanthates are particularly appealing for additive manufacturing because of the resulting high polymerization rates and greater oxygen-tolerance compared to trithiocarbonate-mediated photoiniferter polymerizations. Rapid photolysis leads to quenching of radicals by oxygen, therefore oxygen is less of a concern due to the high concentration of radicals in solution. Hartlieb and coworkers demonstrated that by combining the high rates of photolysis of xanthates with the high degrees of chain transfer of trithiocarbonates, efficient multiblock copolymers could be synthesized under open-to-air conditions at more rapid rates than by using trithiocarbonates alone [48]. Given the appeal of conducting 3D printing open to air, developments in this field included using xanthates with high-intensity light such that nearly quantitative monomer conversion was achieved in <30 s [95]. The authors demonstrated the self-healing ability of the 3D-printed polymers by cutting the material and re-welding to result in similar material properties to the original film (Fig. 11).

7.3. Dispersed systems

About 20 % of global polymer production is synthesized via dispersed polymerizations [175], and despite the potential challenges of light scattering associated with many heterogeneous systems, photoiniferter polymerization has proven to be viable in dispersed media [176–178]. Boyer and Zetterlund have investigated photoiniferter polymerization in miniemulsion conditions and found that surfactant loading is a crucial parameter in the system [179]. If the concentration of free surfactant in the continuous phase is too high, undesired initiation in the continuous phase (secondary nucleation) occurs, which results in poor molecular weight distributions and low $k_{p,app}$ as a result of the "frustrated entry" phenomenon. As mentioned previously, UHMW polymers can be synthesized via photoiniferter polymerization; however, the high viscosity of the polymerization solution limits processability. The high viscosity generated is widely thought to be necessary for the synthesis of UHMW polymers to reduce termination events [180–182]. To circumvent the high viscosities that accompany UHMW polymerization solutions, miniemulsion conditions have been employed [60,183]. Miniemulsion conditions maintain high viscosity within the droplets but a low reaction mixture viscosity such that the synthesized polymers are far more easily processed. Dispersed systems rely on the confined space and segregation effects which typically result in greater rates of polymerization and higher degrees of polymerization control when compared to homogenous polymerizations [184–186]. Within these systems an additional important aspect to consider is partitioning of the iniferter, particularly the thiocarbonylthio radical that results from photolysis, as this results in fewer control agents per particle leading to a loss of control. To further the potential use of photoiniferter polymerization in miniemulsion conditions, UHMW polymers have recently

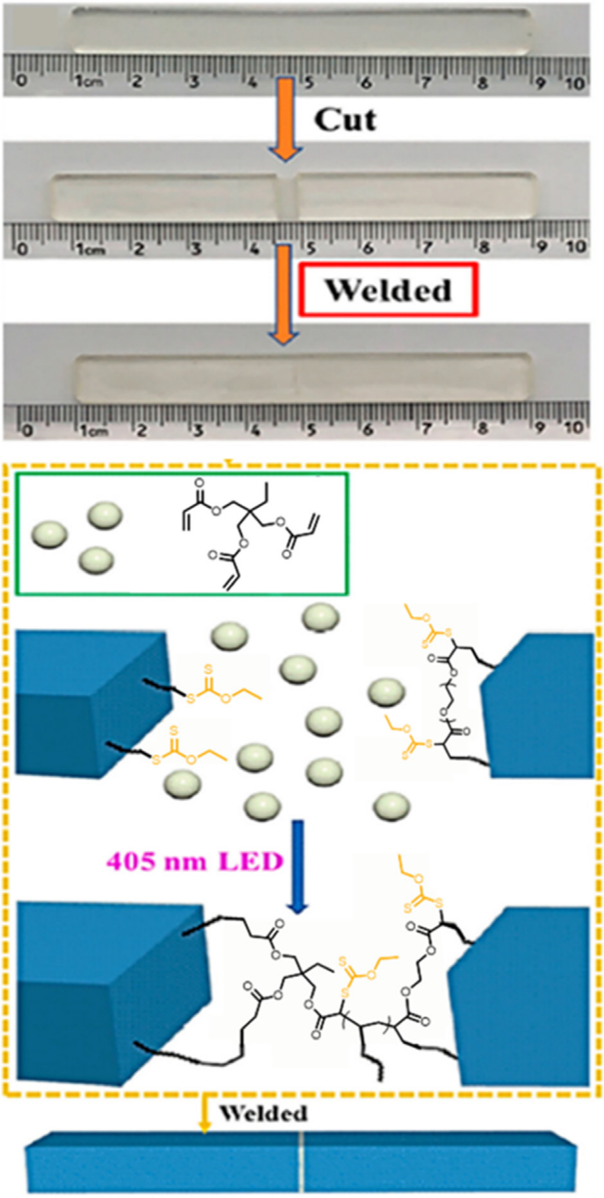

Fig. 11. Photoiniferter polymerization as a means to weld 3D-printed polymers. Adapted with permission from Reference [95]. Copyright© 2022, American Chemical Society.

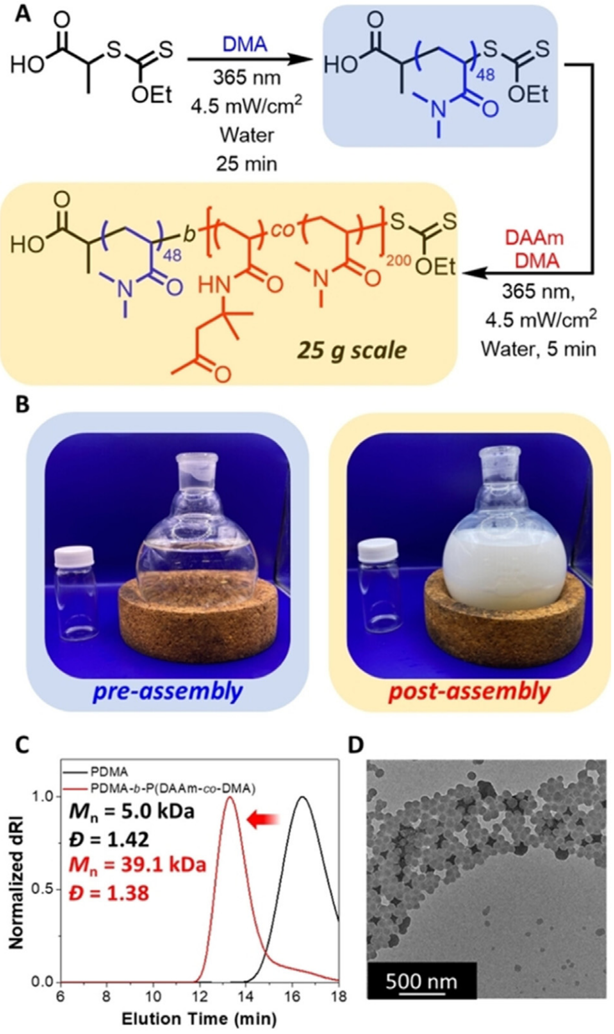

Fig. 12. (A) Reaction scheme of a 25 g scale, one-pot nanoparticle synthesis. (B) The polymerization solution transitioned from clear and homogeneous before PISA (blue) to an opaque, heterogeneous solution after 5 min of UV irradiation (yellow). (C) SEC traces revealed a shift to higher molecular weight upon chain extension of macroiniferter. (D) Spherical micelles were obtained as observed by transmission electron microscopy (TEM) imaging. Adapted with permission from Reference [103]. Copyright© 2023, John Wiley and Sons.

been synthesized in flow, which is promising for the scale-up of this process on an industrial scale [167].

Self-assembled amphiphilic block copolymers have garnered significant interest due to their ability to act as nanocarriers, nanoreactors, and contrast agents [187–190]. In addition to photoiniferter polymerization being used for synthesis in classic dispersed systems, it has also been used to form nanoparticles via polymerization-induced self-assembly (PISA). PISA utilizes a solvophilic polymer which can be chain extended with a solvophilic monomer to create a solvophobic block that self-assembles during polymerization to form nanoparticles [191–193]. Despite the vast majority of work in this area relying on RAFT polymerization to synthesize polymeric nanoparticles [194–200], photoiniferter polymerization is an additional method that has shown promise. One of the first reports on photoiniferter-mediated PISA involved the chain extension of poly(oligoethylene methacrylate) bearing an ω-end trithiocarbonate with benzyl methacrylate using either green or blue light. Well-defined polymeric nanoparticles were formed, albeit after extended reaction times [201]. In another seminal report, O'Reilly and coworkers demonstrated that higher order assemblies were preferentially formed when using photoiniferter polymerization vs RAFT polymerization for PISA due to loss of end-group functionality in the core [202].

One possible drawback of photoiniferter polymerization in PISA is the extended reaction times required compared to photoinitiated-RAFT [203]. To circumvent the high reaction times required for photoiniferter-mediated PISA, Sumerlin and coworkers demonstrated that well-defined nanoparticles could be synthesized in <30 min by leveraging the rapid rates of photolysis of xanthates (Fig. 12) [103]. Alternatively, Zetterlund, Boyer, Junkers, and coworkers have demonstrated that the extended reaction times using trithiocarbonate-mediated photoiniferter polymerization for PISA can be overcome by conducting photoiniferter PISA in flow [204]. Using the designed flow reactor, micelles, worms, and vesicles were obtained from the same batch depending on the degree of polymerization of the core-forming block [204].

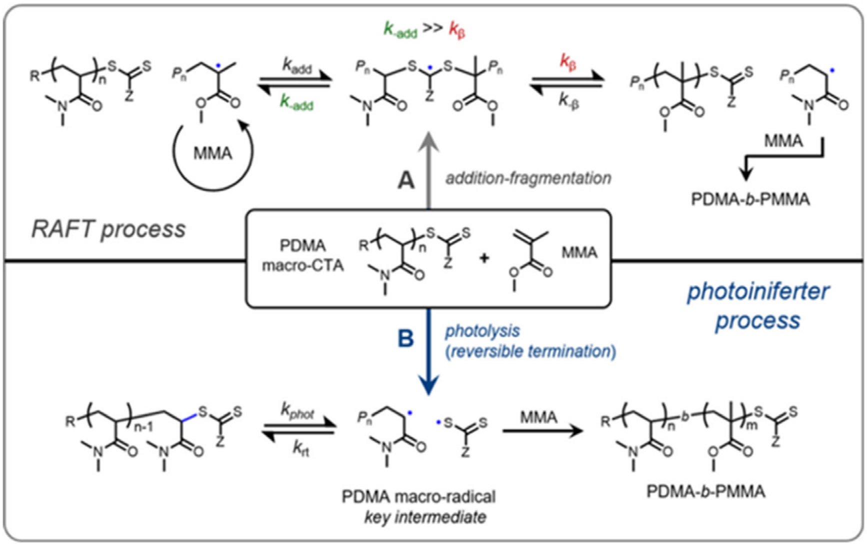

Fig. 13. Pathways outlining mechanistic considerations for block copolymer sequence inversion via RAFT and photoiniferter polymerization. Adapted with permission from Reference [44]. Copyright© 2019, American Chemical Society.

7.4. Sequence control

When preparing block copolymers by RDRP, it is important to consider the blocking sequence. In RAFT polymerization, monomers that form more stabilized radicals are polymerized first and then chain extended with monomers that form less stabilized radicals, a practice that accounts for preferential fragmentation of the intermediate radical formed by chain transfer during the initialization period [99,100]. Reversing the blocking order during RAFT polymerization generally results in poor blocking efficiency and multimodal molecular weight distributions. While inversion of the prescribed polymerization order has been achieved in specialized heterogeneous conditions [205], photoiniferter polymerization allows for the synthesis of reverse-sequence block copolymers under homogenous conditions.

In photoiniferter polymerization, reversed blocking order can be achieved as a consequence of C—S photolysis overcoming the bias of intermediate radical fragmentation to the more stabilized radical. Sumerlin and coworkers reported that inversion of blocking order was most efficient in providing narrow molecular weight distributions when a macro-iniferter bearing a dithiocarbamate or xanthate chain end was used, i.e., when the polymer had endgroups capable of more rapid rates of photolysis than trithiocarbonates (Fig. 13) [44]. The ability to tune the sequence to this degree provides the ability to reach previously unattainable copolymers.

Sequence control of polymers during photoiniferter polymerization methods has also been demonstrated via single-unit monomer insertion (SUMI), such as the report from Aerts et al. [206]. describing the first sequential visible-light-initiated SUMI of *N*,*N*-dimethylacrylamide to 4-((((2-carboxyethyl)thio)carbonothioyl)thio)−4-cyanopentanoic acid in an aqueous solution. The SUMI process was found to be most efficient when using red light. Blue light was also investigated but was less efficient for SUMI, an observation ascribed to a greater extent of photolysis observed when using blue light [206].

8. Conclusions and future directions

While bearing many similarities to RAFT polymerization, photoiniferter polymerization provides an additional approach to well-defined polymers under a wide variety of conditions. Indeed, the renaissance of photoiniferter polymerization represents a significant development in the field of RDRP, offering a versatile and efficient platform for polymer synthesis under mild conditions. Its operational simplicity and compatibility with a variety of monomers echo the strengths of RAFT polymerization but with the added benefits of light-mediated control, offering opportunities for spatial and temporal regulation that are sometimes not as readily achieved via RAFT polymerization. Arguably, some of the advances facilitated by this technique are often overlooked due to inconsistencies in nomenclature, with photoiniferter polymerization frequently being described as a variant of RAFT polymerization, with terms such as "photo-RAFT" or "photoiniferter-RAFT" being adopted. This terminology can obscure the distinct mechanisms of these processes, where RAFT polymerization typically requires an exogenous initiator, whereas photoiniferter polymerization is directly initiated by photolysis of the iniferter itself. A more consistent application of terminology would not only clarify these distinctions but also highlight the unique capabilities of photoiniferter polymerization. Looking forward, the integration of photoiniferter techniques promises to enhance the scope of polymer synthesis, enabling precise control over polymer architecture and functionality while overcoming traditional challenges of achieving well-defined UHMW (co)polymers and prescribed blocking sequences. The ongoing refinement of photoiniferter systems is expected to address current limitations and expand utility in materials science and biotechnology, ultimately leading to innovative materials designed with unprecedented precision.

Declaration of competing interest

The authors declare that they have no known competing financial interests or personal relationships that could have appeared to influence the work reported in this paper.

CRediT authorship contribution statement

Rhys W. Hughes: Writing – review & editing, Writing – original draft, Visualization, Software, Formal analysis, Data curation, Conceptualization. **Megan E. Lott:** Writing – review & editing, Writing – original draft, Visualization, Formal analysis, Data curation, Conceptualization. **Rebecca A. Olson S:** Writing – original draft, Writing – review & editing. **Brent S. Sumerlin:** Writing – original draft, Writing – review & editing.

Data availability

No data was used for the research described in the article.

Acknowledgment

M.E.L. was supported by the Department of Defense (DoD) through the National Defense Science & Engineering Graduate (NDSEG) Fellowship Program.

This material was based on work supported by the DoD through the ARO (W911NF-24–1–0050) and the NSF through DMR-2404144.

References

[1] Ciamician G. The Photochemistry of the Future. Am Assoc Advanc Sci Stable 1912;36:385–94. https://www.jstor.org/stable/1637055.
[2] Chatani S, Kloxin CJ, Bowman CN. The power of light in polymer science: photochemical processes to manipulate polymer formation, structure, and properties. Polym Chem 2014;5:2187–201. doi:10.1039/c3py01334k.
[3] Chen M, Zhong M, Johnson JA. Light-controlled radical polymerization: mechanisms, methods, and applications. Chem Rev 2016;116:10167–211. doi:10.1021/acs.chemrev.5b00671.
[4] Olson RA, Korpusik AB, Sumerlin BS. Enlightening advances in polymer bioconjugate chemistry: light-based techniques for grafting to and from biomacromolecules. Chem Sci 2020;11:5142–56. doi:10.1039/d0sc01544j.
[5] Fairbanks BD, Schwartz MP, Bowman CN, Anseth KS. Photoinitiated polymerization of PEG-diacrylate with lithium phenyl-2,4,6-trimethylbenzoylphosphinate: polymerization rate and cytocompatibility. Biomaterials 2009;30:6702–7. doi:10.1016/j.biomaterials.2009.08.055.
[6] Adzima BJ, Tao Y, Kloxin CJ, DeForest CA, Anseth KS, Bowman CN. Spatial and temporal control of the alkyne–azide cycloaddition by photoinitiated Cu(II) reduction. Nat Chem 2011;3:256–9. doi:10.1038/nchem.980.
[7] Bagheri A. Application of RAFT in 3D printing: where are the future opportunities? Macromolecules 2022. doi:10.1021/acs.macromol.2c02585.
[8] Kannurpatti AR, Anderson KJ, Anseth JW, Bowman CN. Use of “living” radical polymerizations to study the structural evolution and properties of highly crosslinked polymer networks. J Polym Sci B Polym Phys 1997;35:2297–307. doi:10.1002/(SICI)1099-0488(199710)35:14<2297::AID-POLB10>3.0.CO;2-7.
[9] Hartlieb M. Photo-Iniferter RAFT Polymerization. Macromol Rapid Commun 2022;43. doi:10.1002/marc.202100514.
[10] Hughes RW, Lott ME, Bowman JI, Sumerlin BS. Excitation dependence in photoiniferter polymerization. ACS Macro Lett 2022:14–19. doi:10.1021/acsmacrolett.2c00683.
[11] Otsu T, Yoshida M, Tazaki T. A model for living radical polymerization. Macromol Chem Rapid Commun 1982;3:133–40. doi:10.1002/marc.1982.030030209.
[12] Otsu T. Iniferter concept and living radical polymerization. J Polym Sci A Polym Chem 2000;38:2121–36. doi:10.1002/(SICI)1099-0518(20000615)38:12<2121::AID-POLA10>3.0.CO;2-X.
[13] Szwarc M. Living” polymers. Nature 1956;178:1168–9. doi:10.1007/BF00255430.
[14] Tasdelen A, Yagci Y. In: Tsarevsky NV, Sumerlin BS, editors. In Fundamentals of controlled/living radical polymerization. The Royal Society of Chemistry; 2013. p. 78–111. doi:10.1039/9781849737425-00078.
[15] Hill MR, Carmean RN, Sumerlin BS. Expanding the scope of RAFT polymerization: recent advances and new horizons. Macromolecules 2015;48:5459–69. doi:10.1021/acs.macromol.5b00342.
[16] Perrier S. 50th anniversary perspective: RAFT polymerization - a user guide. Macromolecules 2017;50:7433–47. doi:10.1021/acs.macromol.7b00767.
[17] Storey RF. In: Tsarevsky NV, Sumerlin BS, editors. fundamental aspects of living polymerization. The Royal Society of Chemistry; 2013. p. 60–77. doi:10.1039/9781849737425-00060.
[18] Kennedy JP, Smith RA. New telechelic polymers and sequential copolymers by polyfunctional initiator-transfer agents (inifers). II. Synthesis and characterization of α,ω-di(tert-chloro)polyisobutylenes. J Polym Sci: Polym Chem 1980;18:1523–37. doi:10.1002/pol.1980.170180509.
[19] Kennedy JP, Hiza M. New telechelic polymers and sequential copolymers by polyfunctional initiator-transfer agents (Inifers). Polym Bull 1982;8:557–62. doi:10.1007/BF00262935.
[20] Santos R, Kennedy Joseph P, Walters M. New telechelic polymers and sequential copolymers by polyfunctional initiator-transfer agents (INIFERS). Polym Bull 1984;11:261–7. doi:10.1007/BF00255350.
[21] Nicolas J, Guillaneuf Y, Lefay C, Bertin D, Gigmes D, Charleux B. Nitroxide-mediated polymerization. Prog Polym Sci 2013;38:63–235. doi:10.1016/j.progpolymsci.2012.06.002.
[22] Hawker CJ, Bosman AW, Harth E. New polymer synthesis by nitroxide mediated living radical polymerizations. Chem Rev 2001;101:3661–88. doi:10.1021/cr990119u.
[23] Grubbs RB. Nitroxide-mediated radical polymerization: limitations and versatility. Polym Rev 2011;51:104–37. doi:10.1080/15583724.2011.566405.
[24] Studer A, Schulte T. Nitroxide-mediated radical processes. Chemical Record 2005;5:27–35. doi:10.1002/tcr.20033.
[25] Matyjaszewski K. Atom transfer radical polymerization: from mechanisms to applications. Isr J Chem 2012;52:206–20. doi:10.1002/ijch.201100101.
[26] Lou Q, Shipp DA. Recent developments in atom transfer radical polymerization (ATRP): methods to reduce metal catalyst concentrations. ChemPhysChem 2012;13:3257–61. doi:10.1002/cphc.201200166.
[27] Whitfield R, Anastasaki A, Nikolaou V, Jones GR, Engelis NG, Discekici EH, et al. Universal conditions for the controlled polymerization of acrylates, methacrylates, and styrene via Cu(0)-RDRP. J Am Chem Soc 2017;139:1003–10. doi:10.1021/jacs.6b11783.
[28] Matyjaszewski K. Atom Transfer Radical Polymerization (ATRP): current status and future perspectives. Macromolecules 2012;45:4015–39. doi:10.1021/ma3001719.
[29] Lorandi F, Fantin M, Matyjaszewski K. Atom transfer radical polymerization: a mechanistic perspective. J Am Chem Soc 2022;144:15413–30. doi:10.1021/jacs.2c05364.
[30] Dworakowska S, Lorandi F, Gorczyński A, Matyjaszewski K. Toward green atom transfer radical polymerization: current status and future challenges. Adv Sci 2022;9. doi:10.1002/advs.202106076.
[31] Haddleton DM, Clark AJ, Crossman MC, Duncalf DJ, Heming AM, Morsley SR, et al. Atom transfer radical polymerisation (ATRP) of methyl methacrylate in the presence of radical inhibitors. ChemComm 1997:1173–4. doi:10.1039/a702166f.
[32] Truong NP, Jones GR, Bradford KGE, Konkolewicz D, Anastasaki A. A comparison of RAFT and ATRP methods for controlled radical polymerization. Nat Rev Chem 2021;5:859–69. doi:10.1038/s41570-021-00328-8.
[33] Nothling MD, Fu Q, Reyhani A, Allison-Logan S, Jung K, Zhu J, Kamigaito M, et al. Progress and perspectives beyond traditional RAFT polymerization. Adv Sci 2020;7:1–12. doi:10.1002/advs.202001656.
[34] Moad G, Rizzardo E, Thang SH. RAFT polymerization and some of its applications. Chem Asian J 2013;8:1634–44. doi:10.1002/asia.201300262.
[35] Moad G. RAFT polymerization to form stimuli-responsive polymers. Polym Chem 2017;8:177–219. doi:10.1039/c6py01849a.
[36] Boyer C, Bulmus V, Davis TP, Ladmiral V, Liu J, Perrier S. Bioapplications of RAFT polymerization. Chem Rev 2009;109:5402–36. doi:10.1021/cr9001403.
[37] Semsarilar M, Abetz V. Polymerizations by RAFT: developments of the technique and its application in the synthesis of Tailored (Co)polymers. Macromol Chem Phys 2021;222. doi:10.1002/macp.202000311.
[38] Tian X, Ding J, Zhang B, Qiu F, Zhuang X, Chen Y. Recent advances in RAFT polymerization: novel initiation mechanisms and optoelectronic applications. Polymers 2018;10. doi:10.3390/polym10030318.
[39] Barner-Kowollik C, Perrier S. The future of reversible addition fragmentation chain transfer polymerization. J Polym Sci A Polym Chem 2008;46:5715–23. doi:10.1002/pola.22866.
[40] Lamontagne HR, Lessard BH. Nitroxide-mediated polymerization: a versatile tool for the engineering of next generation materials. ACS Appl Polym Mater 2020;2:5327–44. doi:10.1021/acsapm.0c00888.
[41] Matyjaszewski K, Xia J. Atom transfer radical polymerization. Chem Rev 2001;101:2921–90. doi:10.1021/cr940534g.
[42] Moad G, Chiefari J, Chong YK, Krstina J, Mayadunne RT, Postma A, et al. Living free radical polymerization with reversible addition-fragmentation chain transfer (the life of RAFT). Polym Int 2000;49:993–1001. doi:10.1002/1097-0126(200009)49:9<993::AID-PI506>3.0.CO;2-6.
[43] Moad G, Rizzardo E, Thang SH. Living radical polymerization by the RAFT process A second update. Aust J Chem 2009;62:1402–72. doi:10.1071/CH09311.
[44] Easterling CP, Xia Y, Zhao J, Fanucci GE, Sumerlin BS. Block copolymer sequence inversion through photoiniferter polymerization. ACS Macro Lett 2019;8:1461–6. doi:10.1021/acsmacrolett.9b00716.
[45] Lehnen A-C, Kurki JAM, Hartlieb M. The difference between photo-iniferter and conventional RAFT polymerization: high livingness enables the straightforward synthesis of multiblock copolymers. Polym Chem 2022;13:1537–46. doi:10.1039/d1py01530c.
[46] Figg CA, Hickman JD, Scheutz GM, Shanmugam S, Carmean RN, Tucker BS, et al. Color-coding visible light polymerizations to elucidate the activation of trithiocarbonates using eosin y. Macromolecules 2018;51:1370–6. doi:10.1021/acs.macromol.7b02533.
[47] Doi T, Matsumoto A, Otsu T. Elucidation of mechanism for living radical polymerization of styrene with N,N-diethyldithiocarbamate derivatives as iniferters by the use of spin trapping technique. J Polym Sci A Polym Chem 1994;32:2241–9. doi:10.1002/pola.1994.080321205.
[48] Lehnen A-C, Gurke J, Bapolisi AM, Reifarth M, Bekir M, Hartlieb M. Xanthate-supported photo-iniferter (XPI)-RAFT polymerization: facile and rapid access to complex macromolecules. Chem Sci 2023. doi:10.4324/9781003117711-5.
[49] McKenzie TG, Fu Q, Wong EHH, Dunstan DE, Qiao GG. Visible light mediated controlled radical polymerization in the absence of exogenous radical sources or catalysts. Macromolecules 2015;48:3864–72. doi:10.1021/acs.macromol.5b00965.
[50] Barner-Kowollik C, Davis TP, Heuts JPA, Stenzel MH, Vana P, Whittaker M. RAFTing down under: tales of missing radicals, fancy architectures, and mysterious holes. J Polym Sci A Polym Chem 2003;41:365–75. doi:10.1002/pola.10567.
[51] Donovan MS, Sanford TA, Lowe AB, Sumerlin BS, Mitsukami Y, McCormick CL. RAFT Polymerization of N, N -Dimethylacrylamide in Water. Macromolecules 2002;35:4570–2. doi:10.1021/ma020191l.
[52] Smith AE, Xu X, McCormick CL. Stimuli-responsive amphiphilic (co)polymers via RAFT polymerization. Prog Polym Sci 2010;35:45–93. doi:10.1016/j.progpolymsci.2009.11.005.

[53] Convertine AJ, Ayres N, Scales CW, Lowe AB, McCormick CL. Facile, controlled, room-temperature RAFT polymerization of N -Isopropylacrylamide. Biomacromolecules 2004;5:1177–80. doi:10.1021/bm049825h.

[54] Li S, Han G, Zhang W. Photoregulated reversible addition-fragmentation chain transfer (RAFT) polymerization. Polym Chem 2020;11:1830–44. doi:10.1039/d0py00054j.

[55] Li X, Wang L, Chen G, Haddleton DM, Chen H. Visible light induced fast synthesis of protein-polymer conjugates: controllable polymerization and protein activity. ChemComm 2014;50:6506–8. doi:10.1039/c4cc02277g.

[56] Allegrezza ML, Konkolewicz D. PET-RAFT polymerization: mechanistic perspectives for future materials. ACS Macro Lett 2021;10:433–46. doi:10.1021/acsmacrolett.1c00046.

[57] Lee Y, Boyer C, Kwon MS. Photocontrolled RAFT polymerization: past, present, and future. Chem Soc Rev 2023;52:3035–97. doi:10.1039/d1cs00069a.

[58] Kwon MS, Yu C, Ha JK, Ahn J, Lee J, Choi J, Chang T, et al. Defect-free acrylic polymers with a near-Poisson distribution prepared via catalyst-free visible-light-driven radical polymerization. Chemrxiv 2023. doi:10.26434/chemrxiv-2023-dl842.

[59] Carmean RN, Becker TE, Sims MB, Sumerlin BS. Ultra-high molecular weights via aqueous reversible-deactivation radical polymerization. Chem 2017;2:93–101. doi:10.1016/j.chempr.2016.12.007.

[60] Olson RA, Lott ME, Garrison JB, Davidson CLG, Trachsel L, Pedro DI, Sawyer WG, Sumerlin BS. Inverse miniemulsion photoiniferter polymerization for the synthesis of ultra-high molecular weight polymers. Macromolecules 2022;55:8451–60. doi:10.1021/acs.macromol.2c01239.

[61] Carmean RN, Sims MB, Figg CA, Hurst PJ, Patterson JP, Sumerlin BS. Ultrahigh molecular weight hydrophobic acrylic and styrenic polymers through organic-phase photoiniferter-mediated polymerization. ACS Macro Lett 2020;9:613–18. doi:10.1021/acsmacrolett.0c00203.

[62] Otsu T, Yamaguchi M. Metal-Containing Initiator Systems. III. Polymerization of Styrene by Some Activated Metals in the Presence of Organic Halides. Bull Chem Soc Jpn 1968;41:2931–5. doi:10.1246/bcsj.41.2931.

[63] Otsu T, Tazaki T. Living radical polymerization in homogeneous system with phenylazotriphenylmethane as a thermal iniferter. Polym Bull 1986;16:277–84. doi:10.1007/BF00254997.

[64] Mak AM, Steudel R, Wong MW. Homolytic SS bond dissociation of 11 bis(thiocarbonyl)disulfides R-C(=S)-S-S-C(=S)R and prediction of A novel rubber vulcanization accelerator. Chem Asian J 2008;3:1026–34. doi:10.1002/asia.200800036.

[65] Lalevée J, El-Roz M, Allonas X, Fouassier JP. Controlled photopolymerization reactions: the reactivity of new photoiniferters. J Polym Sci A Polym Chem 2007;45:2436–42. doi:10.1002/pola.22005.

[66] Moad G. RAFT polymerization – then and now. ACS Sympos Ser 2015;1187:211–46. doi:10.1021/bk-2015-1187.ch012.

[67] Corrigan N, Jung K, Moad G, Hawker CJ, Matyjaszewski K, Boyer C. Reversible-deactivation radical polymerization (Controlled/living radical polymerization): from discovery to materials design and applications. Prog Polym Sci 2020;111:101311. doi:10.1016/j.progpolymsci.2020.101311.

[68] Braunecker WA, Matyjaszewski K. Controlled/living radical polymerization: features, developments, and perspectives. Prog Polym Sci 2007;32:93–146. doi:10.1016/j.progpolymsci.2006.11.002.

[69] Kumar M, Kannan T. A novel tertiary bromine-functionalized thermal iniferter for controlled radical polymerization. Polym J 2010;42:916–22. doi:10.1038/pj.2010.92.

[70] Beres MA, Rho JY, Kerr A, Smith T, Perrier S. Photoiniferter-RAFT polymerization mediated by bis(trithiocarbonate) disulfides. Polym Chem 2024. doi:10.1039/d3py01307c.

[71] Odian G. Radical chain polymerization. In: Principles of polymerization, Wiley-Interscience. John Wiley & Sons, Inc; 1970. p. 279–300. doi:10.1002/047147875X.ch3.

[72] Zhou H, Johnson JA. Photo-controlled growth of telechelic polymers and end-linked polymer gels. Angew Chem Int Ed 2013;52:2235–8. doi:10.1002/ange.201207966.

[73] Wang H, Li Q, Dai J, Du F, Zheng H, Bai R. Real-time and in situ investigation of “living”/controlled photopolymerization in the presence of a trithiocarbonate. Macromolecules 2013;46:2576–82. doi:10.1021/ma400208j.

[74] Irshadeen IM, Walden SL, Wegener M, Truong VX, Frisch H, Blinco JP, et al. Action plots in action: in-depth insights into photochemical reactivity. J Am Chem Soc 2021;143:21113–26. doi:10.1021/jacs.1c09419.

[75] Walden SL, Carroll JA, Unterreiner A, Barner-Kowollik C. Photochemical action plots reveal the fundamental mismatch between absorptivity and photochemical reactivity. Adv Sci 2024;11. doi:10.1002/advs.202306014.

[76] Gauci SC, Du Prez FE, Holloway JO, Houck HA, Barner-Kowollik C. The power of action plots: unveiling reaction selectivity of light-stabilized dynamic covalent chemistry. Angew Chem Int Ed 2023;62:e202310274. doi:10.1002/anie.202310274.

[77] Kasha M, McGlynn SP. Molecular electronic spectroscopy. Annu Rev Phys Chem 1956;7:403–24. https://www.annualreviews.org/content/journals/10.1146/annurev.pc.07.100156.002155.

[78] Tian G, Xu J, Rao L. Optical absorption and structure of a highly symmetrical Neptunium(V) Diamide COMPLEX. Angew Chem Int Ed 2005;44:6200–3. doi:10.1002/ange.200501281.

[79] Rizzo G, Blasi D, Ragni R, Farinola GM. New insights in luminescent fluorinated transition metal compounds. Adv Organomet Chem 2022;78:189–231. doi:10.1016/bs.adomc.2022.05.001.

[80] Pietrzyk DJ, Frank CW. Qualitative analysis: ultraviolet, visible, and infrared. Anal Chem 1979:410–24. doi:10.1016/B978-0-12-555160-1.50022-8.

[81] Arrington KJ, Matson JB. Assembly of a visible light photoreactor: an inexpensive tool for bottlebrush polymer synthesis: via photoiniferter polymerization. Polym Chem 2017;8:7452–6. doi:10.1039/c7py01741c.

[82] Coyle JD. The photochemistry of thiocarbonyl compounds. Tetrahedron 1985;41:5393–425. doi:10.1016/S0040-4020(01)91341-9.

[83] De Mayo P. Thione photochemistry, and the chemistry of the S2 State. Acc Chem Res 1976;9:52–9. doi:10.1021/ar50098a002.

[84] Fox RB. Photophysical processes and their role in polymer photochemistry. Pure Appl Chem 1972;30:87–104. doi:10.1351/pac197230010087.

[85] Allegrezza ML, De Alwis Watuthanthrige N, Wang Y, Garcia GA, Ren H, Konkolewicz D. Substituent effects in iniferter photopolymerization: can bond homolysis be enhanced by electronics? Polym Chem 2020;11:6129–33. doi:10.1039/d0py01086c.

[86] Li J, Zhang M, Zhu J, Zhu X. Investigation into the Direct Photolysis Process of Photo-Induced RAFT Polymerization by ESR Spin Trapping. Polym J 2019;11:1722.

[87] Wood JH, Bost RW. Sulfur studies. XI. Some sulfur derivatives of Benzaldehyde. J Am Chem Soc 1937;59:1011–13. doi:10.1021/ja01285a015.

[88] George PD. Participation of carbon disulfide in the Friedel-crafts reaction. J Org Chem 1961;26:4235–8. doi:10.1021/jo01069a015.

[89] Hedgley EJ, Fletcher HG. Synthesis of a Thionobenzoate in the Polyhydroxytetrahydropyran series. J Org Chem 1965;30:1282–3. doi:10.1021/jo01015a530.

[90] Liu Y, He J, Xu J, Fan D, Tang W, Yang Y. Thermal decomposition of cumyl dithiobenzoate. Macromolecules 2005;38:10332–5. doi:10.1021/ma0513970.

[91] Tauer K, Nozari S, Imroz Ali AM. Experimental reconsideration of radical entry into latex particles. Macromolecules 2005;38:8611–13. doi:10.1021/ma0510385.

[92] Quinn JF, Barner L, Barner-Kowollik C, Rizzardo E, Davis TP. Reversible addition−fragmentation chain transfer polymerization initiated with ultraviolet radiation. Macromolecules 2002;35:7620–7. doi:10.1021/ma0204296.

[93] Carmean RN, Figg CA, Scheutz GM, Kubo T, Sumerlin BS. Catalyst-free Photoinduced end-group removal of thiocarbonylthio functionality. ACS Macro Lett 2017;6:185–9. doi:10.1021/acsmacrolett.7b00038.

[94] Lu L, Zhang H, Yang N, Cai Y. Toward rapid and well-controlled ambient temperature RAFT polymerization under UV - Vis radiation: effect of radiation wave range. Macromolecules 2006;39:3770–6. doi:10.1021/ma060157x.

[95] Zhao B, Li J, Xiu Y, Pan X, Zhang Z, Zhu J. Xanthate-Based photoiniferter RAFT polymerization toward oxygen-tolerant and rapid living 3D printing. Macromolecules 2022;55:1620–8. doi:10.1021/acs.macromol.1c02521.

[96] Shanmugam S, Cuthbert J, Kowalewski T, Boyer C, Matyjaszewski K. Catalyst-free selective photoactivation of RAFT polymerization: a facile route for preparation of Comblike and bottlebrush polymers. Macromolecules 2018;51:7776–84. doi:10.1021/acs.macromol.8b01708.

[97] McKenzie TG, Da Costa LPM, Fu Q, Dunstan DE, Qiao GG. Investigation into the photolytic stability of RAFT agents and the implications for photopolymerization reactions. Polym Chem 2016;7:4246–53. doi:10.1039/c6py00808a.

[98] Aydogan C, Yilmaz G, Shegiwal A, Haddleton DM, Yagci Y. Photoinduced controlled/living polymerizations. Angew Chem Int Ed 2022;61:e202117377. doi:10.1002/ange.202117377.

[99] Chiefari J, Mayadunne RTA, Moad CL, Moad G, Rizzardo E, Postma A, et al. Thiocarbonylthio Compounds(S = C(Z)S-R) in free radical polymerization with reversible addition-fragmentation chain transfer (RAFT Polymerization). Effect of the activating group Z. Macromolecules 2003;36:2273–83.

[100] Chong BYK, Krstina J, Le TPT, Moad G, Postma A, Rizzardo E, et al. Thiocarbonylthio compounds [S=C(Ph)S-R) in free radical polymerization with reversible addition-fragmentation chain transfer (RAFT polymerization). Role of the free-radical leaving group (R). Macromolecules 2003;36:2256–72. doi:10.1021/ma020882h.

[101] Blokker E, Brink M, van der Schuur JM, Hamlin TA, Bickelhaupt FM. Origin of the Captodative Effect: the Lone-Pair Shielded Radical. Chem Eur 2023;1:1–8. doi:10.1002/ceur.202300006.

[102] Moad G. A critical survey of dithiocarbamate reversible addition-fragmentation chain transfer (RAFT) agents in radical polymerization. J Polym Sci A Polym Chem 2019;57:216–27. doi:10.1002/pola.29199.

[103] Bowman JI, Eades CB, Vratsanos MA, Gianneschi NC, Sumerlin BS. Ultrafast Xanthate-Mediated Photoiniferter polymerization-induced self-assembly (PISA). Angew Chem Int Ed 2023;62:e202309951. doi:10.1002/anie.202309951.

[104] Wanasinghe SV, Sun M, Yehl K, Cuthbert J, Matyjaszewski K, Konkolewicz D. PET-RAFT Increases uniformity in polymer networks. ACS Macro Lett 2022;11:1156–61. doi:10.1021/acsmacrolett.2c00448.

[105] Bradford KGE, Petit LM, Whitfield R, Anastasaki A, Barner-Kowollik C, Konkolewicz D. Ubiquitous nature of rate retardation in reversible addition-fragmentation chain transfer polymerization. J Am Chem Soc 2021;143:17769–77. doi:10.1021/jacs.1c08654.

[106] Haven JJ, Junkers T. Mapping dithiobenzoate-mediated RAFT polymerization products via online microreactor/mass spectrometry monitoring. Polymers 2018;10:1–14. doi:10.3390/polym10111228.

[107] Benaglia M, Chiefari J, Chong YK, Moad G, Rizzardo E, Thang SH. Universal (Switchable) RAFT agents. J Am Chem Soc 2009;131:6914–15. doi:10.1021/ja901955n.

[108] Opiyo G, Jin J. Recent progress in switchable RAFT agents: design, synthesis and application. Eur Polym J 2021;159:110713. doi:10.1016/j.eurpolymj.2021.110713.

[109] Ma Q, Qiao GG, An Z. Visible light photoiniferter polymerization for dispersity control in high molecular weight polymers. Angew Chem Int Ed 2023;62:e202314729. doi:10.1002/anie.202314729.

[110] Xia YN, Scheutz GM, Easterling CP, Zhao JP, Sumerlin BS. Hybrid block copolymer synthesis by merging photoiniferter and organocatalytic ring-opening polymerizations. Angew Chem Int Ed 2021;60:18537–41. doi:10.1002/anie.202106418.

[111] Xu J, Shanmugam S, Corrigan NA, Boyer C. Catalyst-free visible light-induced RAFT photopolymerization. In: Controlled Radical Polymerization: Mechanisms, Chap. 13, ACS Editors. Matyjaszewski, K; 2015. p. 247–67. doi:10.1021/bk-2015-1187.ch013.

[112] Lauterbach F, Rubens M, Abetz V, Junkers T. Ultrafast PhotoRAFT block copolymerization of isoprene and styrene facilitated through continuous-flow operation. Angew Chem Int Ed 2018;57:14260–4. doi:10.1002/anie.201809759.

[113] Rubens M, Latsrisaeng P, Junkers T. Visible light-induced iniferter polymerization of methacrylates enhanced by continuous flow. Polym Chem 2017;8:6496–505. doi:10.1039/C7PY01157A.

[114] Li C-Y, Yu S-S. Efficient visible-light-driven RAFT polymerization mediated by deep eutectic solvents under an open-to-Air environment. Macromolecules 2021;54:9825–36. doi:10.1021/acs.macromol.1c01367.

[115] Quinn JF, Rizzardo E, Barner L, Barner-Kowollik C, Davis TP. Reversible addition-fragmentation chain transfer polymerization initiated with ultraviolet and γ radiation. Macromolecules 2002;35:7620–7.

[116] Wu D, Hong C, Pan C, He W. Study on controlled radical alternating copolymerization of styrene with maleic anhydride under UV irradiation. Polym Int 2003;52:98–103. doi:10.1002/pi.1039.

[117] Ramakers G, Rubens M, Krivcov A, Möbius H, Trouillet V, Welle A, et al. Photoiniferter surface grafting of poly(methyl acrylate) using xanthates. J Polym Sci A Polym Chem 2019;57:2002–7. doi:10.1002/pola.29405.

[118] Khan MY, Cho MS, Kwark YJ. Dual roles of a xanthate as a radical source and chain transfer agent in the photoinitiated RAFT polymerization of vinyl acetate. Macromolecules 2014;47:1929–34. doi:10.1021/ma5002244.

[119] Otsu T, Matsunaga T, Doi T, Matsumoto A. Features of living radical polymerization of vinyl monomers in homogeneous system using N,N-diethyldithiocarbamate derivatives as photoiniferters. Eur Polym J 1995;31:67–78. doi:10.1016/0014-3057(94)00122-7.

[120] Garrison JB, Hughes RW, Sumerlin BS. Backbone degradation of polymethacrylates via metal-free ambient-temperature photoinduced single-electron transfer. ACS Macro Lett 2022;11:441–6. doi:10.1021/acsmacrolett.2c00091.

[121] Makino H, Nishikawa T, Ouchi M. Incorporation of a boryl pendant as the trigger in a methacrylate polymer for backbone degradation. ChemComm 2022;58:11957–60. doi:10.1039/d2cc04882e.

[122] Kimura T, Ouchi M. Photocatalyzed hydrogen atom transfer degradation of Vinyl polymers: cleavage of a backbone C−C Bond triggered by radical activation of a C−H Bond in a pendant. Angew Chem Int Ed 2023;62:e202305252. doi:10.1002/anie.202305252.

[123] Smith RA, Fu G, McAteer O, Xu M, Gutekunst WR. Radical approach to Thioester-containing polymers. J Am Chem Soc 2019;141:1446–51. doi:10.1021/jacs.8b12154.

[124] Shieh P, Zhang W, Husted KEL, Kristufek SL, Xiong B, Lundberg DJ, et al. Cleavable comonomers enable degradable, recyclable thermoset plastics. Nature 2020;583:542–7. doi:10.1038/s41586-020-2495-2.

[125] Ko K, Lundberg DJ, Johnson AM, Johnson JA. Mechanism-guided discovery of cleavable comonomers for backbone Deconstructable Poly(methyl methacrylate). J Am Chem Soc 2024;146:9142–54. doi:10.1021/jacs.3c14554.

[126] Liu P, Jimaja S, Immel S, Thomas C, Mayer M, Weder C, et al. Mechanically triggered on-demand degradation of polymers synthesized by radical polymerizations. Nat Chem 2024;16:1184–92. doi:10.1038/s41557-024-01508-x.

[127] Hughes RW, Marquez JD, Young JB, Garrison JB, Zastrow IS, Evans AM, et al. Selective electrochemical modification and degradation of polymers. Angew Chem Int Ed 2024;202403026:1–7. doi:10.1002/anie.202403026.

[128] Lin Y, Kouznetsova TB, Craig SL. Mechanically gated degradable polymers. J Am Chem Soc 2020;142:2105–9. doi:10.1021/jacs.9b13359.

[129] Hill MR, Kubo T, Goodrich SL, Figg CA, Sumerlin BS. Alternating radical ring-opening polymerization of cyclic ketene acetals: access to tunable and functional polyester copolymers. Macromolecules 2018;51:5079–84. doi:10.1021/acs.macromol.8b00889.

[130] Albanese KR, Morris PT, de Alaniz JR, Bates CM, Hawker CJ. Controlled-radical polymerization of αlipoic acid: a general route to degradable Vinyl copolymers. J Am Chem Soc 2023;145:22728–34. doi:10.1021/jacs.3c08248.

[131] Hughes RW, Lott ME, Zastrow IS, Young JB, Maity T, Sumerlin BS. Bulk Depolymerization of methacrylate polymers via pendent group activation. J Am Chem Soc 2024;146:6217–24. doi:10.1021/jacs.3c14179.

[132] De Luca Bossa F, Yilmaz G, Matyjaszewski K. Fast Bulk Depolymerization of Polymethacrylates by ATRP. ACS Macro Lett 2023;12:1173–8. doi:10.1021/acsmacrolett.3c00389.

[133] Martinez MR, Schild D, De Luca Bossa F, Matyjaszewski K. Depolymerization of Polymethacrylates by Iron ATRP. Macromolecules 2022;55:10590–9. doi:10.1021/acs.macromol.2c01712.

[134] Martinez MR, De Luca Bossa F, Olszewski M, Matyjaszewski K. Copper(II) Chloride/Tris(2-pyridylmethyl)amine-Catalyzed Depolymerization of Poly(n-butyl methacrylate). Macromolecules 2022;55:78–87. doi:10.1021/acs.macromol.1c02246.

[135] Martinez MR, Dadashi-Silab S, Lorandi F, Zhao Y, Matyjaszewski K. Depolymerization of P(PDMS11MA) bottlebrushes via atom transfer radical polymerization with activator regeneration. Macromolecules 2021;54:5526–38. doi:10.1021/acs.macromol.1c00415.

[136] Wang HS, Truong NP, Jones GR, Anastasaki A. Investigating the effect of end-group, molecular weight, and solvents on the catalyst-free Depolymerization of RAFT polymers: possibility to reverse the polymerization of heat-sensitive polymers. ACS Macro Lett 2022;11:1212–16. doi:10.1021/acsmacrolett.2c00506.

[137] Whitfield R, Jones GR, Truong NP, Manring LE, Anastasaki A. Solvent-free chemical recycling of Polymethacrylates made by ATRP and RAFT polymerization: high-yielding depolymerization at low temperatures. Angew Chem Int Ed 2023;62:e202309116. doi:10.1002/anie.202309116.

[138] Flanders MJ, Gramlich WM. Reversible-addition fragmentation chain transfer (RAFT) mediated depolymerization of brush polymers. Polym Chem 2018;9:2328–35. doi:10.1039/c8py00446c.

[139] Wang HS, Truong NP, Pei Z, Coote ML, Anastasaki A. Reversing RAFT polymerization: near-quantitative monomer generation via a catalyst-free Depolymerization approach. J Am Chem Soc 2022;144:4678–84. doi:10.1021/jacs.2c00963.

[140] Young JB, Bowman JI, Eades CB, Wong AJ, Sumerlin BS. Photoassisted radical Depolymerization. ACS Macro Lett 2022;11:1390–5. doi:10.1021/acsmacrolett.2c00603.

[141] Bellotti V, Parkatzidis K, Wang HS, De Alwis Watuthanthrige N, Orfano M, Monguzzi A, et al. Light-accelerated depolymerization catalyzed by Eosin Y. Polym Chem 2022;14:253–8. doi:10.1039/d2py01383e.

[142] Young JB, Hughes RW, Tamura AM, Bailey LS, Stewart KA, Sumerlin BS. Bulk depolymerization of poly (methyl methacrylate) via chain-end initiation for catalyst-free reversion to monomer. Chem 2023;9:1–14. doi:10.1016/j.chempr.2023.07.004.

[143] Lohmann V, Jones GR, Truong NP, Anastasaki A. The thermodynamics and kinetics of depolymerization: what makes vinyl monomer regeneration feasible? Chem Sci 2024. doi:10.1039/d3sc05143a.

[144] Jones GR, Wang HS, Parkatzidis K, Whitfield R, Truong NP, Anastasaki A. Reversed controlled polymerization (RCP): depolymerization from well-defined polymers to monomers. J Am Chem Soc 2023;145:9898–915. doi:10.1021/jacs.3c00589.

[145] Häfliger F, Truong NP, Wang HS, Anastasaki A. Fate of the RAFT End-group in the thermal depolymerization of polymethacrylates. ACS Macro Lett 2023;12:1207–12. doi:10.1021/acsmacrolett.3c00418.

[146] Wang HS, Parkatzidis K, Junkers T, Truong NP, Anastasaki A. Controlled radical depolymerization: structural differentiation and molecular weight control. Chem 2023;10:388–401. doi:10.1016/j.chempr.2023.09.027.

[147] Bellotti V, Wang HS, Truong NP, Simonutti R, Anastasaki A. Temporal regulation of PET-RAFT controlled radical depolymerization. Angew Chem Int Ed 2023;62:1–6. doi:10.1002/anie.202313232.

[148] Parkatzidis K, Wang HS, Truong NP, Anastasaki A. Recent developments and future challenges in controlled radical polymerization: a 2020 update. Chem 2020;6:1575–88. doi:10.1016/j.chempr.2020.06.014.

[149] An Z. 100th anniversary of macromolecular science viewpoint: achieving ultrahigh molecular weights with reversible deactivation radical polymerization. ACS Macro Lett 2020;9:350–7. doi:10.1021/acsmacrolett.0c00043.

[150] Rzayev J, Penelle J. HP-RAFT: a free-radical polymerization technique for obtaining living polymers of ultrahigh molecular weights. Angew Chem Int Ed 2004;43:1691–4. doi:10.1002/anie.200353025.

[151] Gong H, Gu Y, Zhao Y, Quan Q, Han S, Chen M. Precise synthesis of ultrahigh-molecular-weight fluoropolymers enabled by chain-transfer-agent differentiation under visible-light irradiation. Angew Chem Int Ed 2020;59:919–27. doi:10.1002/anie.201912698.

[152] Diodati LE, Wong AJ, Lott ME, Carter AG, Sumerlin BS. Unraveling the Properties of Ultrahigh Molecular Weight Polyacrylates. ACS Appl Polym Mater 2023;5:9714–20. doi:10.1021/acsapm.3c02191.

[153] Kwak Y, Nicolaÿ R, Matyjaszewski K. Synergistic interaction between ATRP and RAFT: taking the best of each world. Aust J Chem 2009;62:1384. doi:10.1071/CH09230.

[154] Jakubowski W, Kirci-Denizli B, Gil RR, Matyjaszewski K. Polystyrene with improved chain-end functionality and higher molecular weight by ARGET ATRP. Macromol Chem Phys 2008;209:32–9. doi:10.1002/macp.200700425.

[155] Kwak Y, Matyjaszewski K. Photoirradiated atom transfer radical polymerization with an Alkyl Dithiocarbamate at ambient temperature. Macromolecules 2010;43:5180–3. doi:10.1021/ma100850a.

[156] Nicolaÿ R, Kwak Y, Matyjaszewski K. A green route to well-defined high-molecular-weight (Co)polymers Using ARGET ATRP with Alkyl Pseudohalides and copper catalysis. Angew Chem Int Ed 2010;49:541–4. doi:10.1002/anie.200905340.

[157] Read E, Guinaudeau A, Wilson DJ, Cadix A, Violleau F, Destarac M. Low temperature RAFT/MADIX gel polymerisation: access to controlled ultrahigh molar mass polyacrylamides. Polym Chem 2014;5:2202–7. doi:10.1039/c3py01750h.

[158] Matyjaszewski K. Advanced materials by atom transfer radical polymerization. Adv Mater 2018;30. doi:10.1002/adma.201706441.

[159] Li R, An Z. Achieving ultrahigh molecular weights with diverse architectures for unconjugated monomers through Oxygen-Tolerant Photoenzymatic RAFT polymerization. Angew Chem Int Ed 2020;59:22258–64. doi:10.1002/anie.202010722.

[160] Kamiyama Y, Tamate R, Hiroi T, Samitsu S, Fujii K, Ueki T. Highly stretchable and self-healable polymer gels from physical entanglements of ultrahigh–molecular weight polymers. Sci Adv 2022;8. doi:10.1126/sciadv.add0226.

[161] Wylie RAL, Jafari VF, Qiao GG. Photoiniferter RAFT accelerated by ionic liquids in organic solvent systems. Macromolecules 2023. doi:10.1021/acs.macromol.3c02346.

[162] Santha Kumar ARS, Allison-Logan S, Finnegan JR, Singha NK, Ashokkumar M, Qiao G. Visible light-accelerated Photoiniferter polymerization in ionic liquid. ACS Macro Lett 2023;12:1012–18. doi:10.1021/acsmacrolett.3c00329.

[163] Perrier S, Davis TP, Carmichael AJ, Haddleton DM. First report of reversible addition – fragmentation chain transfer (RAFT) polymerisation in room temperature ionic liquids The Reversible Addition – fragmentation chain Transfer (RAFT) polymerisation of acrylates, methacrylates and ionic liquids ; th. ChemComm 2002:2226–7.

[164] Streicher M, Boyko V, Blanazs A. Ultra-high-Molecular-weight, narrow-polydispersity polyacrylamides synthesized using photoiniferter polymerization to generate high-performance flocculants. ACS Appl Mater Interfaces 2023;15:59044–54. doi:10.1021/acsami.3c14483.

[165] Arita T, Kayama Y, Ohno K, Tsujii Y, Fukuda T. High-pressure atom transfer radical polymerization of methyl methacrylate for well-defined ultrahigh molecular-weight polymers. Polymer 2008;49:2426–9. doi:10.1016/j.polymer.2008.03.026.

[166] Bernat R, Szczepaniak G, Kamiński K, Paluch M, Matyjaszewski K, Maksym P. Visible-light-induced ATRP under high-pressure: synthesis of ultra-high-molecular-weight polymers. ChemComm 2023:843–6. doi:10.1039/d3cc04982e.

[167] Davidson CLG, Lott ME, Trachsel L, Wong AJ, Olson RA, Pedro DI, Sawyer WG, Sumerlin BS. Inverse Miniemulsion enables the continuous-flow synthesis of controlled ultra-high molecular weight polymers. ACS Macro Lett 2023;12:1224–30. doi:10.1021/acsmacrolett.3c00431.

[168] Trachsel L, Konar D, Hillman JD, Davidson CLG, Sumerlin BS. Diversification of acrylamide polymers via direct transamidation of unactivated tertiary amides. J Am Chem Soc 2024;146:1627–34. doi:10.1021/jacs.3c12174.

[169] Trachsel L, Stewart KA, Konar D, Hillman JD, Moerschel JA. Sumerlin BS. β-Triketones as reactive handles for polymer diversification via dynamic Catalyst-free Diketoenamine click chemistry. J Am Chem Soc 2024;146:16257–67. doi:10.1021/jacs.4c04664.

[170] Albanese KR, Okayama Y, Morris PT, Gerst M, Gupta R, Speros JC, et al. Building tunable degradation into high-performance Poly(acrylate) pressure-sensitive adhesives. ACS Macro Lett 2023;12:787–93. doi:10.1021/acsmacrolett.3c00204.

[171] Bobrin VA, Yao Y, Shi X, Xiu Y, Zhang J, Corrigan N, et al. Nano- to macro-scale control of 3D printed materials via polymerization induced microphase separation. Nat Commun 2022;13:1–10. doi:10.1038/s41467-022-31095-9.

[172] Jung K, Corrigan N, Ciftci M, Xu J, Seo SE, Hawker CJ, et al. Designing with light: advanced 2D, 3D, and 4D materials. Adv Mater 2020;32:1–21. doi:10.1002/adma.201903850.

[173] Zhang Z, Corrigan N, Bagheri A, Jin J, Boyer C. A versatile 3D and 4D printing system through Photocontrolled RAFT polymerization. Angew Chem Int Ed 2019;58:17954–63. doi:10.1002/anie.201912608.

[174] Bagheri A, Engel KE, Bainbridge CWA, Xu J, Boyer C, Jin J. 3D printing of polymeric materials based on photo-RAFT polymerization. Polym Chem 2020;11:641–7. doi:10.1039/c9py01419e.

[175] Jasinski F, Zetterlund PB, Braun AM, Chemtob A. Photopolymerization in dispersed systems. Prog Polym Sci 2018;84:47–88. doi:10.1016/j.progpolymsci.2018.06.006.

[176] Shim SE, Shin Y, Jun JW, Lee K, Jung H, Choe S. Living-free-radical emulsion Photopolymerization of methyl methacrylate by a surface active Iniferter (Suriniferter). Macromolecules 2003;36:7994–8000. doi:10.1021/ma034331i.

[177] Jung K, Xu J, Zetterlund PB, Boyer C. Visible-light-regulated controlled/living radical polymerization in miniemulsion. ACS Macro Lett 2015;4:1139–43. doi:10.1021/acsmacrolett.5b00576.

[178] Huang Z, Qiu T, Xu H, Shi H, Rui J, Li X, et al. Surfactant-free visible-light-controlled emulsion polymerization toward ABA-type amphiphilic triblock copolymers. Macromolecules 2018;51:7329–37. doi:10.1021/acs.macromol.8b01523.

[179] Jung K, Boyer C, Zetterlund PB. RAFT iniferter polymerization in miniemulsion using visible light. Polym Chem 2017;8:3965–70. doi:10.1039/c7py00939a.

[180] Brooks BW. Viscosity effects in the free-radical polymerization of Methyl methacrylate. Proc R Soc Lond, Ser A, Math Phys Sci 1977;357:183–92. doi:10.1098/rspa.1977.0162.

[181] North AM, Reed GA. Diffusion-controlled termination during the initial stages of free radical polymerization of methyl methacrylate. Trans Faraday Soc 1961;57:859–70. doi:10.1039/TF9615700859.

[182] Shipp DA, Matyjaszewski K. Kinetic analysis of controlled/'living' radical polymerizations by simulations. 1. The importance of diffusion-controlled reactions. Macromolecules 1999;32:2948–55. doi:10.1021/ma9819135.

[183] Lott ME, Trachsel L, Schué E, Davidson CLG, Olson SRA, Pedro DI, et al. Ultrahigh-molecular-weight Triblock copolymers via inverse miniemulsion photoiniferter polymerization. Macromolecules 2024. doi:10.1021/acs.macromol.4c00366.

[184] Zetterlund PB, Kagawa Y, Okubo M. Controlled/living radical polymerization in dispersed systems. Chem Rev 2008;108:3747–94. doi:10.1021/cr800242x.

[185] Zetterlund PB, Thickett SC, Perrier S, Bourgeat-Lami E, Lansalot M. Controlled/living radical polymerization in dispersed systems: an update. Chem Rev 2015;115:9745–800. doi:10.1021/cr500625k.

[186] Engelis NG, Anastasaki A, Nurumbetov G, Truong NP, Nikolaou V, Shegiwal A, et al. Sequence-controlled methacrylic multiblock copolymers via sulfur-free RAFT emulsion polymerization. Nat Chem 2017;9:171–8. doi:10.1038/NCHEM.2634.

[187] Mable CJ, Canton I, Mykhaylyk OO, Ustbas Gul B, Chambon P, Themistou E, et al. Targeting triple-negative breast cancer cells using Dengue virus-mimicking pH-responsive framboidal triblock copolymer vesicles. Chem Sci 2019;10:4811–21. doi:10.1039/c8sc05589k.

[188] Esser L, Truong NP, Karagoz B, Moffat BA, Boyer C, Quinn JF, et al. Gadolinium-functionalized nanoparticles for application as magnetic resonance imaging contrast agents: via polymerization-induced self-assembly. Polym Chem 2016;7:7325–37. doi:10.1039/c6py01797e.

[189] Blackman LD, Varlas S, Arno MC, Fayter A, Gibson MI, O'Reilly RK. Permeable protein-loaded polymersome cascade nanoreactors by polymerization-induced self-assembly. ACS Macro Lett 2017;6:1263–7. doi:10.1021/acsmacrolett.7b00725.

[190] Blackman LD, Varlas S, Arno MC, Houston ZH, Fletcher NL, Thurecht KJ, et al. Confinement of therapeutic enzymes in selectively permeable polymer vesicles by polymerization-induced self-assembly (PISA) reduces antibody binding and proteolytic susceptibility. ACS Cent Sci 2018;4:718–23. doi:10.1021/acscentsci.8b00168.

[191] Liu C, Hong CY, Pan CY. Polymerization techniques in polymerization-induced self-assembly (PISA). Polym Chem 2020;11:3673–89. doi:10.1039/d0py00455c.

[192] Bowman JI, Eades CB, Korpanty J, Garrison JB, Scheutz GM, Goodrich SL, et al. Controlling morphological transitions of polymeric nanoparticles via doubly responsive block copolymers. Macromolecules 2023;56:3316–23. doi:10.1021/acs.macromol.3c00445.

[193] Scheutz GM, Bowman JI, Mondal S, Rho JY, Garrison JB, Korpanty J, et al. Gradient copolymer synthesis through self-assembly. ACS Macro Lett 2023;12:454–61. doi:10.1021/acsmacrolett.3c00148.

[194] Canning SL, Smith GN, Armes SP. A critical appraisal of RAFT-mediated polymerization-induced self-assembly. Macromolecules 2016;49:1985–2001. doi:10.1021/acs.macromol.5b02602.

[195] Wan J, Fan B, Thang SH. RAFT-mediated polymerization-induced self-assembly (RAFT-PISA): current status and future directions. Chem Sci 2022;13:4192–224. doi:10.1039/d2sc00762b.

[196] Ikkene D, Six JL, Ferji K. Progress in aqueous dispersion RAFT PISA. Eur Polym J 2023;188:111848. doi:10.1016/j.eurpolymj.2023.111848.

[197] Warren NJ, Armes SP. Polymerization-induced self-assembly of block copolymer nano-objects via RAFT aqueous dispersion polymerization. J Am Chem Soc 2014;136:10174–85. doi:10.1021/ja502843f.

[198] Wang J, Hu X, Zhu N, Guo K. Continuous flow photo-RAFT and light-PISA. Chem Eng J 2021;420:127663. doi:10.1016/j.cej.2020.127663.

[199] Tkachenko V, Matei Ghimbeu C, Vaulot C, Vidal L, Poly J, Chemtob A. RAFT-photomediated PISA in dispersion: mechanism, optical properties and application in templated synthesis. Polym Chem 2019;10:2316–26. doi:10.1039/c9py00209j.

[200] Yeow J, Boyer C. Photoinitiated polymerization-induced self-assembly (Photo-PISA): new insights and opportunities. Adv Sci 2017;4. doi:10.1002/advs.201700137.

[201] Yeow J, Sugita OR, Boyer C. Visible light-mediated polymerization-induced self-assembly in the absence of external catalyst or initiator. ACS Macro Lett 2016;5:558–64. doi:10.1021/acsmacrolett.6b00235.

[202] Blackman LD, Doncom KEB, Gibson MI, RK O'Reilly. Comparison of photo- and thermally initiated polymerization-induced self-assembly: a lack of end group fidelity drives the formation of higher order morphologies. Polym Chem 2017;8:2860–71. doi:10.1039/c7py00407a.

[203] Tan J, Sun H, Yu M, Sumerlin BS, Zhang L. Photo-PISA: shedding light on polymerization-induced self-assembly. ACS Macro Lett 2015;4:1249–53. doi:10.1021/acsmacrolett.5b00748.

[204] Zaquen N, Yeow J, Junkers T, Boyer C, Zetterlund PB. Visible light-mediated polymerization-induced self-assembly using continuous flow reactors. Macromolecules 2018;51:5165–72. doi:10.1021/acs.macromol.8b00887.

[205] Khan M, Guimarães TR, Choong K, Moad G, Perrier S, Zetterlund PB. RAFT emulsion polymerization for (Multi)block copolymer synthesis: overcoming the constraints of monomer order. Macromolecules 2021;54:736–46. doi:10.1021/acs.macromol.0c02415.

[206] Aerts A, Lewis RW, Zhou Y, Malic N, Moad G, Postma A. Light-induced RAFT single unit monomer insertion in aqueous solution—toward sequence-controlled polymers. Macromol Rapid Commun 2018;39:1–7. doi:10.1002/marc.201800240.